

Holocene sedimentary systems on a broad continental shelf with abundant river input: process–product relationships

SHU GAO*, DANDAN WANG, YANG YANG, LIANG ZHOU, YANGYANG ZHAO,
WENHUA GAO, ZHUOCHEN HAN, QIAN YU & GAOCONG LI

*Ministry of Education Key Laboratory for Coast and Island Development,
Nanjing University, Nanjing 210093, China*

*Corresponding author (e-mail: shugao@nju.edu.cn)

Abstract: The region consisting of the Bohai, Yellow and East China seas represents a typical wide continental shelf environment with abundant terrestrial sediment supply. Here, a variety of sedimentary systems have been formed during the Holocene period. These systems have unique characteristics in terms of spatial distribution, material composition, deposition rate, and the timing and duration for their formation, which are related to active sediment-transport processes induced by tides and waves, shelf circulations, and sediment gravity flows. The sedimentary records contained within the deposits have a high temporal resolution, but each with a limited temporal coverage. However, if these records are connected, then they may form a complete archive for environmental change studies. In the field of process–product relationship studies, the mid-Holocene coastal deposits on the Jiangsu coast, the early–middle Holocene sequences of the Hangzhou Bay, the Holocene mud deposits off the Zhejiang–Fujian coasts and the other mud areas over the region are of importance. These systems may be understood by identifying the material supply (from both seabed reworking during the sea-level rise events and river discharges), transport–accumulation processes, the formation of sediment sequences and the future evolution of the sediment systems, for which numerical modelling becomes increasingly important.

Sedimentary archives on continental shelves contain environmental information related to sea-level changes. Ever since the time of Charles Lyell, it has been proposed that the temporal scale of sedimentary sequences can be determined by using the global sea-level curve. For example, Sloss (1963) suggested that there have been six major sea-level cycles since the Cambrian and that these provide a general chronological control for stratigraphic sequences. Subsequently, Vail *et al.* (1977), in an attempt to establish correlations between the sequence and sea-level position on smaller temporal scales, presented a novel global eustatic chart. The most direct application of this new approach is to interpret the stratigraphic characteristics of shallow-marine deposits in terms of time periods covered by the deposits, and to infer possible hiatuses on the basis of known sea-level curves. The sea-level chart has been modified by a number of authors (e.g. Haq *et al.* 1987), to be widely used as a standard tool for sequence stratigraphic analysis.

However, in using the global eustatic chart, only one factor, namely the sea-level position, was emphasized; other important factors such as the initial bathymetry, sediment supply and transport–accumulation processes were largely neglected. As a result, the global eustatic chart is only able to predict the timing of sedimentary sequences, whereas

the spatial extent of sedimentary systems cannot be determined. Such an analysis would be sufficient if an investigation were merely connected with macro-scale temporal changes (Kamp & Naish 1998; Paola 2000). However, when smaller timescales are considered (e.g. the formation and evolution of Holocene shelf–coastal sedimentary systems), then the other factors cannot be neglected. Sloss (1963) actually suggested that, in addition to sea level, the three factors listed above were important, but he did not proceed to analyse the combined influences of all four factors. Over the years, measurements of sediment dynamics on decadal scales were carried out in an attempt to relate the product of the sedimentary environments (i.e. the sedimentary sequences and archives) to the controlling processes (Nittrouer & Wright 1994; Nittrouer *et al.* 2009). Furthermore, scientific research programmes such as Strataform were developed to illuminate process–product relationships (Nittrouer 1999).

In terms of the initial bathymetric conditions at a fixed sea level, the width and bed slope of the shelf is a result of tectonic and sedimentological evolution; while, the terrestrial sediment input influences the sediment budget of the shelf. In combination, these two factors can generate four different shelf types: (1) wide shelves with abundant

sediment supply (e.g. the shelves of the Bohai, Yellow and East China seas); (2) narrow shelves with abundant sediment supply (e.g. the Bengal Bay); (3) wide sediment-starved shelves (e.g. the North Sea in Europe); and (4) narrow shelves with poor sediment supply (e.g. the shelves along the western North American coastline). Furthermore, these two factors also influence the hydrodynamics and, hence, the sediment-transport capacity. Three major processes can be distinguished: tide-induced transport (often in combination with wave action); fine-grained sediment transport due to shelf circulations; and sediment gravity flows (Gao & Collins 2014). Thus, different types of continental shelves will generate different sedimentary systems, resulting in different types of sedimentary archives or records in terms of their resolution, continuity and duration, all of which are important for past global change studies.

The purpose of the present contribution is to synthesize the characteristics of the Holocene

sedimentary systems of the Bohai, Yellow and East China seas, including their temporal evolution and spatial distribution patterns, and the resultant sedimentary records, from the point of view of sediment dynamics. The study area, which is characterized by a gentle bed slope and abundant sediment supply, is associated with rich sediment archives for environmental change research. Hence, it would be desirable to elucidate the relationships between the processes and products in order to provide a basis of appropriate stratigraphic interpretation. In addition, some critical scientific problems needing attention in the future are identified.

Regional environmental setting

The region covering the Bohai, Yellow and East China seas is characterized by a wide shelf with abundant terrestrial sediment supply (Fig. 1). Covering a total area of some $1.26 \times 10^6 \text{ km}^2$, the region

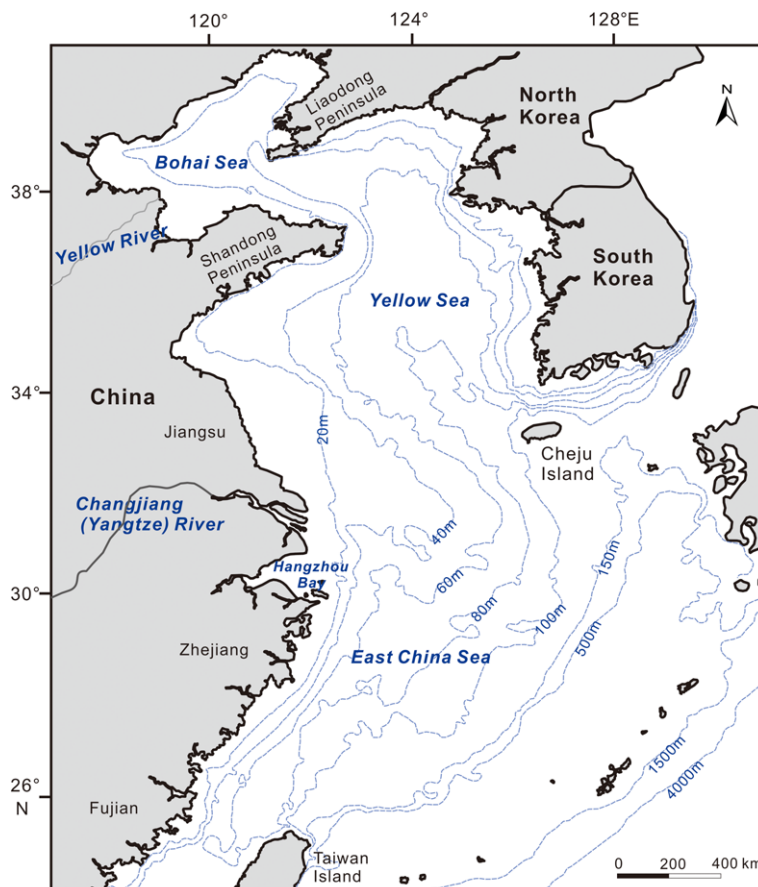


Fig. 1. Geographical setting of the study area (bathymetry in metres).

in consideration receives large sediment inputs from the Yellow and Changjiang rivers, as well as from numerous smaller rivers. As a result, large river deltas and other types of shelf–coastal deposits are formed. The Holocene mud deposits are representative of such an environmental setting (Fig. 2). Here, the river discharges are two magnitudes higher than those of the North Sea in Europe; such a magnitude of sediment supply favours the formation of shelf mud deposits (Dronkers & Miltenburg 1996). The reason for this is that in a closed system the repeated resuspension and settling would not result in overall net deposition, but only redistribution of the sedimentary material within the system; only when there is an external source can

net accretion take place. Thus, the high sediment discharge, induced by the regional monsoon climate, meets the condition for the formation of deposits on a large scale.

The Yellow River is well known for its high sediment load over the entire Holocene period. Because this river discharged alternatively into the Bohai and southern Yellow seas during the late Holocene, two large deltas were formed (Chen & Zhu 2012). One is located on the coast of the Bohai Sea, with the most recent part having formed since 1855 and covering an area of around $6 \times 10^3 \text{ km}^2$. The other is the Old Yellow River delta on the Jiangsu coast, which formed in the period from AD 1128 to AD 1855, when the river discharged into the

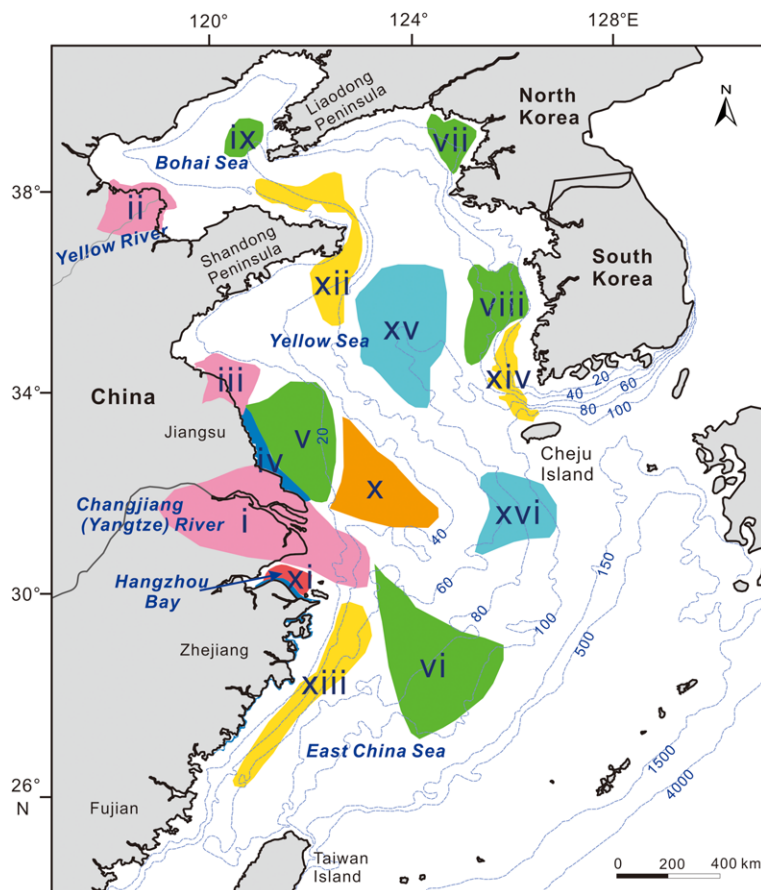


Fig. 2. Distribution of major coastal and shelf Holocene sedimentary systems over the study area: (i) Changjiang River delta; (ii) Yellow River delta; (iii) the abandoned delta associated with the Old Yellow River; (iv) tidal flats on the Jiangsu coast; (v) Jiangsu radial tidal ridges; (vi) palaeo-tidal ridges on the East China Sea shelf; (vii) tidal ridges off the North Korean coast; (viii) tidal ridges off the South Korean coast; (ix) tidal ridges in the Bohai Sea; (x) Yangtze Shoal; (xi) Hangzhou Bay estuarine deposit; (xii) Yellow River distal mud; (xiii) Changjiang distal mud; (xiv) Huskan Mud Belt in the SE Yellow Sea; (xv) isolated mud patch in the central Yellow Sea; and (xvi) isolated mud patch to the south of Cheju Island (modified from Gao & Collins 2014).

southern Yellow Sea; this delta originally covered an area of some $12 \times 10^3 \text{ km}^2$, which has been subject to coastal erosion after the river mouth shifted to the north. The Changjiang River delta has a sub-aerial area of $25 \times 10^3 \text{ km}^2$ and a subaqueous delta of $10 \times 10^3 \text{ km}^2$ (cf. Gao 2007). In addition, the deposits of adjacent areas (e.g. the Hangzhou Bay) are also influenced by the input of the Changjiang River. It should be noted that the suspended sediment from the large rivers may be transported over long distance to form distal mud deposits such as those around the Shandong Peninsula, northern Yellow Sea, associated with the Yellow River (J. P. Liu *et al.* 2004), and offshore of the Zhejiang–Fujian coast, associated with the Changjiang River (J. P. Liu *et al.* 2007; Xu *et al.* 2009). The fine-grained sediment may be further dispersed towards the middle or outer shelf, where it forms isolated mud patches (Gao & Jia 2003). Along the west coast of Korea, thick Holocene mud deposits were emplaced, the material probably having different sources, although Korean researchers generally favour the small local rivers as the main source (Park *et al.* 2000; Lee & Chu 2001).

As a typical broad, sediment-starved continental shelf environment, the North Sea in Europe is characterized by tidal ridges, tidal sand sheets, tidal flats and barrier island lagoon systems (Flemming & Davis 1994; Collins *et al.* 1995). These Holocene deposits are mainly a product of the reworking of early sedimentary bodies by waves and tidal currents during the post-glacial transgression. Similar deposits are distributed over the eastern China shelf regions, including the tidal-ridge fields in the eastern Bohai Sea and off the Jiangsu coast (the SW Yellow Sea) (Liu *et al.* 1998; Y. Wang *et al.* 2012), as well as off the western coast of Korea (Off 1963), the Yangtze Shoal to the NE of the Changjiang River mouth (Liu 1997) and the palaeo-tidal ridges on the middle–outer shelf of the East China Sea (to the SE of the Changjiang Estuary) (Yang 1989; Z. X. Liu *et al.* 2007). These deposits have resulted from the modification to the underlying strata over the course of the Holocene.

The region is characterized by a monsoon climate: that is, northerly winds prevail in winter but southerly winds are dominant in summer. During the winter, cold outbreaks occur, with winter storms hitting the coasts; in the summer time, the region is often influenced by typhoons, which represent a major natural hazard. The waves are moderate, except during storm events. The tides are mainly semi-diurnal in character, with the largest ranges being observed on the opposite coasts of both sides of the Yellow Sea, the maximum range reaching 9.39 m on the Jiangsu coast, SW Yellow Sea (Ding *et al.* 2014), and in Hangzhou Bay, where large-scale tidal bores occur (Fan *et al.* 2014).

Sediment-transport and accumulation processes

Tidally induced sediment transport

Tides in this region play an important role in sediment transport. Large tidal ranges and strong tidal currents, in combination with shallow water depths, small seabed slopes and wave action, have resulted in active resuspension and transport of fine-grained sediment. Figure 3 shows the spatial and seasonal distribution patterns of suspended sediment over the regions; the high values are mainly due to tidally induced resuspension.

Traditionally, sediment transport in the region was determined from time-series measurements over 26 h at fixed stations, including water depth, current velocity, suspended sediment concentration (SSC), water temperature, salinity and other parameters (Shi 2004). In this way, numerous datasets were collected. Although this method has a large uncertainty in terms of the long-term estimate of sediment fluxes because the measurements may not fully represent the long-term situations, these datasets are invaluable in the analysis of the processes and mechanisms of transport (e.g. resuspension and dispersion/diffusion), and in the modelling of the transport patterns (they provide basic data for parameter determination and model verification). In Table 1, some results of tidal-cycle measurements from inner-shelf areas are listed, which show that the tidal-current velocity is of the order of 1.0 m s^{-1} , the suspended sediment concentration (due to resuspension) has an order of magnitude of $10^{-1} - 10^0 \text{ kg m}^{-3}$, and the resultant sediment-transport rate ranges between 10^{-1} and $10^1 \text{ kg m}^{-1} \text{ s}^{-1}$. In more recent times, longer-term monitoring has been accomplished by means of mooring systems and coastal observatories. For instance, continuous annual measurements of the SSC over the areas adjacent to the Changjiang Estuary have been carried out; the data from several locations indicate that the SSC is controlled by seasonal changes in wave action and river discharges, in addition to tides, which influence the position of the turbidity maxima of the estuarine waters.

The method of numerical modelling has been widely adopted to reveal sediment-transport patterns. For example, suspended-sediment transport has been simulated for the Bohai Sea, the area adjacent to the Yellow River mouth (Jiang *et al.* 2000, 2004; Lu *et al.* 2011), and the Changjiang Estuary and adjoining waters (Chen & Wang 2008; Hu *et al.* 2009). The results obtained indicate that the suspended sediment concentration and its spatial distribution are controlled by tides, but that the long-distance transport of suspended sediment on the shelf is influenced by shelf-circulation patterns.

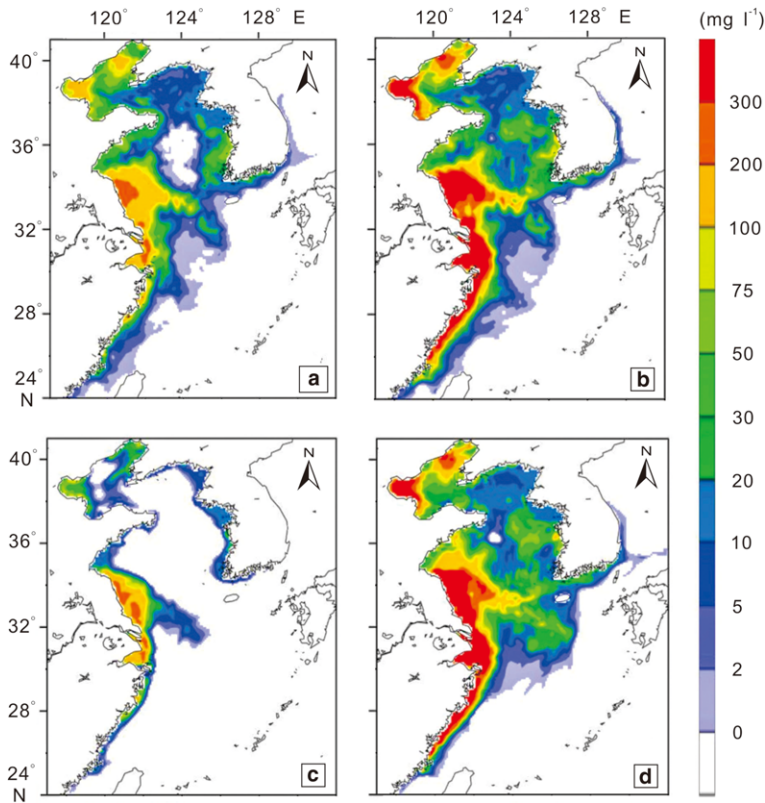


Fig. 3. Model output for suspended sediment concentrations (SSCs) in the study area, where tidal currents are the dominated controlling factor: (a) sea-surface SSCs in January; (b) bottom SSCs in January; (c) sea-surface SSCs in July; and (d) bottom SSCs in July (the colour bar denotes the scale of SSCs in mg l^{-1} , modified from Bian 2012).

For the Jiangsu coast, Xing *et al.* (2012) used the model Mike 12 to calculate the suspended sediment concentration in response to the combined action of waves and tidal currents for both the summer and winter seasons, the results being in good agreement with observational data; furthermore, these authors suggest that the enhancement of resuspension in winter is mainly due to the influence of the reduction in seawater temperature, rather than to the wave effect. In contrast, Wang *et al.* (2011) argued that the intensified wave action in winter plays a significant role. The results of their simulation are consistent with the sediment-transport patterns revealed by satellite imagery, which show sediment dispersal towards the Cheju Island. However, further research is required to resolve certain disagreements between simulation and observation.

Important mechanisms associated with tides include the settling–scour lag effects and time–velocity asymmetry (Postma 1961), which result in net landwards transport. The formation of tidal deposits (e.g. tidal flats and tidal ridges) is

associated with the tidal current in this region (Gao 2009a).

Transport due to currents associated with low-frequency shelf circulations

On the shelf of the Yellow and East China seas, East Asia, which has a width of up to 600 km, circulation includes upwelling induced by the Kuroshio along the shelf edge, monsoon wind-driven currents and water movements related to river discharge (Chen 2009), which results in complicated seasonal patterns (Fig. 4). The general characteristics of the water masses and shelf currents are listed in Table 2. There are a number of mechanisms for the formation of shelf circulations, including: a baroclinic effect (e.g. high-density waters (high salinity, low temperature) intruding onto the shelf in the bottom layer); wind-driven currents (in the case of the monsoon-dominated eastern China seas, with winter and summer winds generating different

Table 1. Tidal-cycle measurements of suspended sediment concentrations and transport rates at some inner-shelf sites of the region

Station	Position	Depth (m)	Current speed (m s^{-1})	SSC (kg m^{-3})	Transport rate ($\text{kg m}^{-1} \text{s}^{-1}$)	References
R10	120° 58.2'	33° 39.7'	15.9	0.70	0.45	5.01
R11	121° 13.7'	33° 19.5'	11.8	0.60	0.21	1.49
Y9	120° 51.8'	33° 10.3'	9.2	0.84	0.89	6.88
Y10	120° 54.63'	33° 11.05'	16.0	0.94	0.55	8.27
Y11	120° 57.9'	32° 58'	8.9	1.04	0.91	8.42
Y12	121° 2.95'	32° 54.2'	6.3	1.09	0.98	6.73
R20	121° 32.6'	32° 57.1'	13.5	0.89	0.10	1.20
Y + 1	121° 08.8'	32° 35'	15.9	0.81	0.29	3.73
Y + 2	121° 19.8'	32° 33'	18.1	0.92	0.21	3.50
R22	121° 44.9'	32° 39.6'	10.8	0.62	0.16	1.07
R23	121° 37'	32° 39.6'	8.1	0.52	0.13	0.55
R24	122° 29.69'	32° 39.6'	17.0	0.76	0.10	1.29
Y13	121° 44.6'	32° 04.6'	5.9	0.58	0.52	1.78
Y14	121° 48.7'	32° 05.4'	7.6	0.72	0.32	1.75
Y15	121° 53'	32° 02'	10.7	0.65	0.13	0.90
Y16	122° 03'	31° 54'	14.7	0.67	0.12	1.18
E2	123° 06'	34° 30'	77.0	0.10	0.03	0.23
A08	120° 48.69'	33° 13.24'	0.4	0.15	0.35	Dong et al. (2011)
M08	120° 49.29'	33° 13.6'	1.7	0.30	0.38	Y. P. Wang et al. (2012)
S1	120° 49.9'	33° 13.93'	4.4	1.00	0.12	0.51
K01	121° 26.58'	32° 53.97'	16.9	0.92	0.16	2.49
K02	121° 32.4'	32° 56.06'	9.6	0.61	0.15	0.85
K03	121° 39'	32° 58.15'	16.4	0.91	0.16	2.39
K04	121° 48.66'	33° 6.52'	18.6	0.99	0.11	2.08
K05	121° 50.04'	33° 0.93'	14.2	0.86	0.14	1.68
K06	121° 54.36'	33° 14.90'	15.8	0.79	0.16	1.99
K07	121° 57.3'	33° 12.10'	19.2	0.83	0.07	1.14
K08	122° 1.2'	33° 6.92'	23.1	0.80	0.05	0.97
K09	122° 3.72'	33° 3.01'	18.1	0.74	0.06	0.77
P01	121° 29.64'	32° 55.22'	11.4	0.92	0.19	1.96
P02	121° 34.26'	32° 56.90'	19.2	0.96	0.14	2.49
YH	122° 34.8'	37° 19.93'	1.5	1.00	0.01	0.02
DF	120° 48.55'	33° 14.12'	1.8	0.35	0.57	Jia et al. (2003)
JB	120° 19.5'	36° 22.98'	7.0	0.30	0.01	Li et al. (2007)
						D. L. Yuan et al. (2008); Y. Yuan et al. (2008)
Tetrapod	121° 51'	31° 12.38'	10.8	1.28	1.30	17.97
JL	118° 01'	24° 25.49'	8.7	1.10	0.02	0.19
A1	119° 3.42'	38° 0.21'	7.0	0.25	0.06	0.10
A2	119° 5.76'	38° 1.15'	11.0	0.40	0.02	0.10
A3	119° 7.5'	38° 1.92'	14.0	0.43	0.22	1.30
A4	119° 10.14'	38° 3.03'	15.0	0.42	0.03	0.20
B1	119° 1.26'	37° 25.87'	5.0	0.22	0.05	0.05
B2	119° 6.3'	37° 28.53'	8.0	0.32	0.04	0.10
B3	119° 10.98'	37° 30.88'	7.0	0.47	0.12	0.40
B4	119° 16.32'	37° 33.70'	5.0	0.35	0.29	0.50
B5	119° 21.18'	37° 36.22'	6.0	0.46	0.40	1.10
C1	119° 10.98'	37° 46.25'	2.7	0.52	0.47	0.66
C2	119° 13.92'	37° 46.56'	2.7	0.54	0.96	Bi et al. (2010) 1.40
C3	119° 17.22'	37° 48.61'	5.0	0.39	0.31	0.60
C4	119° 18.78'	37° 49.86'	12.0	0.53	0.14	0.90
C5	119° 21'	37° 51.58'	15.0	0.41	0.02	0.10
A1	119° 32.46'	26° 4.85'	14.0	0.86	0.16	Li et al. (2009)
A2	119° 37.2'	26° 3.71'	11.0	0.72	0.73	5.78
PHW	119° 14.34'	25° 9.92'	4.9	0.65	0.05	Zhang (2013)

HOLOCENE SEDIMENTARY SYSTEMS

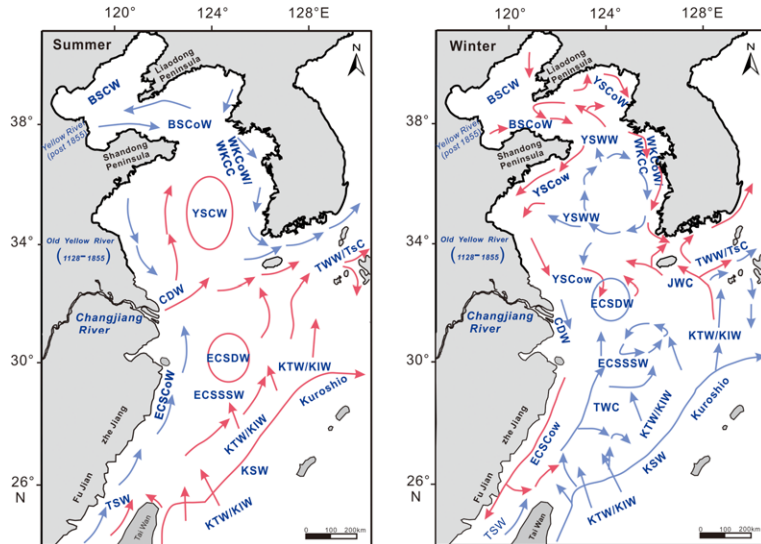


Fig. 4 . Major shelf currents in the summer and winter seasons (compiled on the basis of Chen 2009).

shelf flows); seasonal changes in water temperature that modify the density distributions and thereby trigger water-mass movement; tidal disturbance in shallow waters, generating water masses with different densities from those of the surrounding waters, causing baroclinic movement; and river-derived freshwater inputs, which generate estuarine circulations with river plumes moving seawards in the surface layer.

Fine-grained sediment is transported towards the middle–outer continental shelf, or even across the shelf towards the deep ocean by shelf currents (Liu *et al.* 2006; Yang & Liu 2007). The river-derived sediment can reach the shelf break where it may partially accumulate temporally; when shelf currents permit (e.g. in the East China Sea, where bottom currents flow seawards in winter), the material escapes from the shelf to enter the adjacent

Table 2. General features of major shelf-current and water-mass systems (based on Liu *et al.* 1993; Sun 1995; Hu *et al.* 2000; Chen 2009; W. Li *et al.* 2012; Liu *et al.* 2013)

List of acronyms	Shelf water mass and current systems	Temperature (°C)		Salinity (psu)	
		Winter	Summer	Winter	Summer
BSCW	Bohai Sea Central Water	<1	25–27	<31	<30
BSCoW	Bohai Sea Coastal Water	<3	24–26	30–31	<31.5
CDW	Changjiang Diluted Water	6–17	27–29	20–31	<32
ECSCow	East China Sea Coastal Water	8–17	26–28	25–31	<33.5
ECSDW	East China Sea Dense Water	9–13	27–28	32–34	31.5–33.5
ECSSW	East China Sea Shelf Surface Water	13–18	27–29	34–34.7	33–34.2
JWC	Jeju Warm Current	10–15	25–28	33.5–34.5	31–33
KIW	Kuroshio Intermediate Water	16.5–20.5	14.4–19.5	34.4–34.9	34.4–34.8
KSW	Kuroshio Surface Water	20–24	28–29	33.5–34.75	33.5–34.5
TSW	Taiwan Strait Water	18–23	28–29	33.5–34.5	33.5–34
TWC	Taiwan Warm Current	13–18	28–29	33–34.5	32–34
TsC	Tsushima Current	13–15	27–29	34.5–34.75	33.3–34
TWW	Tsushima Warm Water	12–15	26–28	34.5–34.75	32–33
WKCoW	Western Korea Coastal Current	2–5	20–26	31.5–32.5	<30
YSCoW	Yellow Sea Coastal Water	<4	24–26	31–31.5	<31
YSCW	Yellow Sea Cold Water	5–10	8–10	32–33.5	30.5–31.5
YSWW	Yellow Sea Warm Water	5–12	25–27	32–34	30.5–32
YSWC	Yellow Sea Warm Current	8–13	26.7–27	33–33.5	32.5–33

deep waters (Hoshika *et al.* 2003). On the middle shelf of the Yellow Sea, fine-grained sediment originating from the inner shelf and organic material produced in the water column accumulate in an area with weak tidal currents. Numerical modelling shows that the accumulation may be enhanced by upwelling–downwelling patterns (Gao & Jia 2003). It is interesting to observe that, on the inner shelf of the region, sediment suspended in the surface layer is also transported seawards: remote sensing analysis reveals that the turbid water mass expands into the central Yellow Sea in winter (Shi & Wang 2012). This pattern indicates a fundamental difference between the circulation patterns of wide and narrow shelves. On narrow shelves, seawards flow in the bottom layer would imply landwards flow at the surface, according to mass conservation. However, on wide shelves, the movement of the various water masses creates additional possibilities; for instance, the shelf may be divided into sections, within which vertical circulation patterns may differ.

Sediment movement can be caused by shelf circulation resulting from the combined action of wind, sea-surface gradient and baroclinic effects. Once brought into motion, the flow direction will be influenced by the Coriolis force. The horizontal movement of seawater will inevitably lead to sea-surface elevation changes. The variations in water temperature and salinity at different sites cause horizontal and vertical water-mass movement. As a consequence, the shelf-current system in the region is complex; the complexity is further enhanced by the intrusion of the Kuroshio Current and the freshwater discharge from the Changjiang River (G. X. Li *et al.* 2006; Zhang *et al.* 2007; Chen 2009). Although the flow speed associated with the shelf circulation is much lower than that of the tidal currents (i.e. usually of the order of 1–10 cm s⁻¹; Lee & Chao 2003), long-distance transport of fine-grained sediment nevertheless takes place, even across the entire shelf, because of the low settling velocities of the suspended particles (Nittrouer & Wright 1994).

Suspended-sediment transport in response to shelf circulations has been studied by numerical modelling and *in situ* measurements. In physical oceanography, field, observations and numerical simulations have been carried out for the Kuroshio transport (Hsueh *et al.* 1997), as well as for shelf-circulation patterns (Lee *et al.* 2000), in particular those in the Yellow and East China seas, (Lee *et al.* 2002). On this basis, suspended-sediment transport has been modelled for the entire region (Choi *et al.* 2005).

Along the shelf break of the East China Sea, suspended sediment is transported downslope towards the Okinawa Trough due to localized circulations

cells resulting from the interaction between the Kuroshio core flow and Taiwan island (Sheu *et al.* 1999). According to the data collected during 2000–08, the total amount of suspended sediment in the water column of the Yellow and East China seas in summer reaches 0.18×10^9 t (Dong *et al.* 2011). The quantity is further enhanced in winter due to intensified northerly monsoon winds and waves. For instance, the concentration and the transport rate of suspended sediment in the coastal waters adjacent to the Yellow River mouth are much higher in winter than in summer, with the transport rate being 10^0 – 10^1 kg m⁻¹ s⁻¹ in winter and 10^{-2} – 10^0 kg m⁻¹ s⁻¹ in summer (Yang *et al.* 2011). Under the various hydrodynamic conditions, sediment supplied by the Yellow River can be transported by the shelf current towards the Yellow Sea through the Bohai Strait (Lu *et al.* 2011). On the outer shelf of the East China Sea, suspended cross-shelf sediment transport takes place towards the Okinawa Trough in the form of bottom turbid layer (Watanabe 2007).

An analysis of the MODIS ocean colour imagery (D. L. Yuan *et al.* 2008; Y. Yuan *et al.* 2008; Zhang *et al.* 2010) indicates that the suspended matter distributed over the Yellow and East China seas in winter is derived from the Jiangsu coast, and the seawards dispersion of the suspended sediment is caused by the shelf currents driven by the winter monsoon (Yuan & Hsueh 2010). Furthermore, analyses of the 2002–08 sea-surface temperature, ocean colour, wind speed and sea-surface elevation anomaly data indicate that turbid water, with a concentration of greater than 50 mg l⁻¹, is expanded seawards during January–April, whilst it is confined to the Jiangsu coastal waters during July–September (Shi & Wang 2010, 2012); remote sensing images display the formation of a suspended sediment plume over the Yangtze Shoal, which reveals a transport pathway from the Jiangsu coast towards the middle shelf in winter.

In terms of the processes and mechanisms responsible for the cross-shelf sediment dispersal towards the deep ocean, indirect evidence has been sought from studies on sediment provenance (Yang *et al.* 2003, 2004; Yang & Youn 2007) and the deposition rate of shelf mud (DeMaster *et al.* 1985; Huh & Su 1999; F. Y. Li *et al.* 2006). The method of tracing the provenance is mainly based on the identification of the source and transport pathways from the material deposited at the accumulation site. Many types of tracers – for example, heavy metals (Cu, Pb, Cd) (Lin *et al.* 2002), rare earth elements (Song & Choi 2009), river-derived magnetic minerals (L. B. Wang *et al.* 2009; Zhang *et al.* 2012), clay minerals (Xu *et al.* 2009; Dou *et al.* 2010), chemical index of alteration (CIA) (Yang *et al.* 2002), ²¹⁰Pb and ¹³⁷Cs isotopes

(Chung *et al.* 2003; Du *et al.* 2010), and terrestrial organic matter (Zhu *et al.* 2008) – have been used for this purpose. Thus, the content of Cu, Pb and Cd in the Changjiang sediments has been adopted as tracers to delineate the transport and accumulation on the open shelf and in the Hangzhou Bay, the sedimentary record revealing changes in human activity in the catchment basin (Lin *et al.* 2002). The analysis of clay minerals in the Okinawa Trough, deposited over the last 28 kyr, has revealed the changing patterns of the Changjiang influence: from 28 to 14 ka BP, the sediment is dominated by material supplied by the Changjiang, which is associated with the reworking of shelf deposits during the period of sea-level lowstand from 14 to 8.4 ka BP, followed by material input from Taiwan in the period from 8.4 to 1.5 ka BP and, once again, by material input from the Changjiang over the last 1.5 kyr (Dou *et al.* 2010). Taiwan and the Changjiang clay minerals are both dominated by illite, but the Changjiang sediments have a low crystallinity and a relatively high smectite and kaolinite content; therefore, the sedimentary provenance of the northern Taiwan Strait can be determined based on these differences (Xu *et al.* 2009). After being normalized on the basis of grain-size data, geochemical indices show that the East China Sea material is derived from Chinese rivers; in the Yellow Sea, however, the sediments are supplied from both Chinese and Korean rivers (Lim *et al.* 2006). Many researchers have measured the deposition rate of the shelf mud deposits on the basis of ^{210}Pb and ^{137}Cs dating of cored samples (DeMaster *et al.* 1985; Alexander *et al.* 1991; Huh & Su 1999; F. Y. Li *et al.* 2002; Oguri *et al.* 2003; Lim *et al.* 2007). The results show that near the shoreline the deposition rate is high, reaching levels of $10^0\text{--}10^1 \text{ cm a}^{-1}$, owing to abundant material supply; on most of the open shelf region, the deposition rate is of the order of $10^{-1} \text{ cm a}^{-1}$.

The above studies have identified an interesting discrepancy: according to a simplified model of vertical circulation, the winter monsoon would generate landwards movement in the surface layer and seawards movement in the bottom layer in this particular region (Gao *et al.* 2000), but the satellite imagery indicates seawards dispersion in the surface layer, while, on the outer shelf, the bottom layer is also directed towards the shelf edge (Sheu *et al.* 1999). The mechanisms by which the suspended sediment escapes from the coast and enters the cross-shelf transport system require further investigation. In addition to the wind-induced circulation, various forms of barotropic and baroclinic water-mass movements, together with frontal processes, should be given more attention both in nature and in modelling exercises.

Transport associated with sediment gravity flow

With regard to estuarine and continental shelf sediment gravity flows, the earliest research conducted in this area was for the Yellow River subaqueous delta. The Yellow River was well known for its high suspended sediment concentrations, which favour the formation of hyperpycnal flow: that is, the downslope movement of highly concentrated river waters (Wright *et al.* 1988, 1990). However, the suspended sediment load of the Yellow River has been significantly reduced in the recent times; as a result, the conditions for the development of hyperpycnal flows no longer exist. *In situ* observation shows that downslope movement of suspended sediment today dominantly takes place in bottom turbid layers (Wang *et al.* 2007): that is, bottom water masses with enhanced concentrations in response to resuspension induced by tidal currents and waves. This indicates a regime shift with respect to the nature of sediment gravity flows: hyperpycnal flows are today replaced by mobile bottom turbid layers (Fig. 5). Studies carried out elsewhere (Sternberg *et al.* 1996) show that the movement of turbid bottom layers is a frequent and fundamentally different phenomenon from the classical hyperpycnal flow concept proposed by Wright *et al.* (1990). For example, wave-induced resuspension at the bottom will enhance the density of the bottom layer (because of the addition of suspended mater) and, if the density is higher than the surrounding water mass, will cause downslope movement. Although the suspended sediment concentration of Changjiang River is not as high as that of the Yellow River, intense resuspension resulting from the combined action of waves and tidal currents, and extreme events of typhoons and winter storms, make it an ideal area for sediment gravity flow research (Wright & Friedrichs 2006).

Bottom turbid layers in canyon environments have been taken as indicators of sediment gravity flows (Liu & Lin 2004; Oiwane *et al.* 2011), but, on shelves with gentle slopes, the motion of bottom turbid layers may be linked to the shelf circulation rather than to gravity flows. Honda *et al.* (2000) observed that sediment of low ^{14}C content, which is an indicator of old age, is eroded from the bed and transported into the Okinawa Trough, emphasizing the importance of resuspension events and the formation of bottom turbid layers. Hoshika *et al.* (2003) obtained a time series comprising current velocity over spring–neap tidal cycles, suspended sediment concentration, temperature and salinity measured at three mooring stations at a height of 10 m above the bed in the East China Sea; during the observation period, numerous resuspension and settling events occurred, the authors

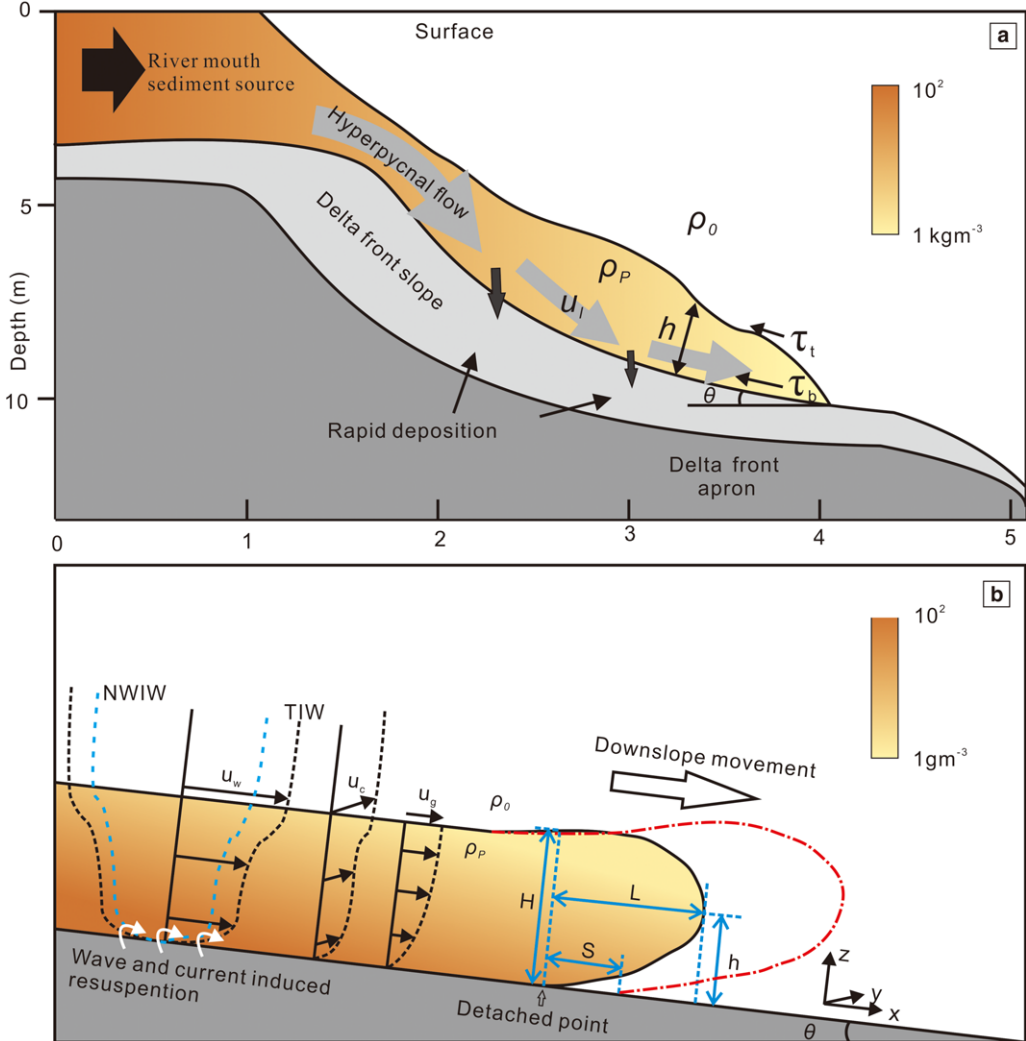


Fig. 5. Types of sediment gravity flows in the study area: (a) hyperpycnal flow near the Yellow River mouth (from Wright *et al.* 1990; Wang *et al.* 2007); and (b) bottom turbid layers formed in response to resuspension processes on the shelf (from Honda *et al.* 2000; Hoshika *et al.* 2003; Oguri *et al.* 2003; Bian *et al.* 2010; Y. H. Li *et al.* 2012). In (a) the colour concentration only shows the order of magnitude of the suspended sediment concentration from Wang *et al.* (2007). Hyperpycnal flow has the thickness H , the speed u and transport direction (grey arrows) in the bed slope θ . τ_t and τ_b represent upper interface and bed shear stress, respectively. In (b) the velocity of the bottom turbid layer is a combination of wave orbital velocity (U_w), along-shelf current magnitude (U_c) and the speed of gravity current (U_g) (Wright *et al.* 2001). U_w has the different ranges of the normal wind-induced wave velocity (NWIW) and the typhoon-induced wave (TIW). The red line represents the downslope variation trend of the BTL.)

associating downslope motion of the bottom turbid layer with circulation driven by monsoon winds. Oguri *et al.* (2003) have made similar observations; in this case, the bottom turbid layer on the East China Sea shelf had suspended sediment concentrations in excess of 20 mg l^{-1} , the downslope movement once again being associated with

wind-driven shelf circulation. However, flow velocities and suspended sediment concentrations measured at mooring stations in the Okinawa Trough and on the continental slope imply that the down-canyon movement of the bottom turbid layer was not associated with tidal currents or other periodic currents, but that the episodic transport was, instead,

characteristic of sediment gravity flow (Chung & Hung 2000). In the Okinawa Trough, the sediment flux is enhanced in winter, indicating an overall influence of the monsoon circulation; within the water column, however, the vertical sediment flux at a height of the 600 m above the bed is considerably weaker than in the turbid layer at the bottom (Iseki *et al.* 2003).

On the inner shelf, extreme events such as typhoons can trigger intense resuspension to generate bottom turbid layers. During a typhoon event that occurred in 2009, the suspended sediment concentration was enhanced significantly in the coastal mud area along the Zhejiang–Fujian coastlines (Y. H. Li *et al.* 2012). On another occasion, bottom turbid layer movement was also observed during a typhoon event in the same area (Bian *et al.* 2010). Observations and modelling of suspended-sediment transport for the Yellow River subaqueous delta reproduced similar process, with the model output showing a significant role being played by the bottom turbid layer to transport fine-grained material towards deep areas (A. J. Wang *et al.* 2010). Apparently, these observations and simulation results have demonstrated the importance of sediment gravity flow, but additional analysis is required to distinguish between the transport effects associated with the turbid layer movement and those in relation to shelf horizontal and vertical circulations.

Formation of major coastal-shelf Holocene deposits

The major sedimentary systems

A variety of Holocene sedimentary systems occur in the study area (Fig. 2). They include river deltas, tidal flats, tidal ridges, and coastal and shelf mud deposits. The geometric features and sedimentary characteristics of these systems are listed in Tables 3 and 4, respectively. Some details of these deposits are described below.

River deltas

The intense river discharges of the Changjiang and Yellow rivers have led to the formation of large deltas (Fig. 6). The Changjiang River delta is the largest Holocene deposit in the region. After sea level reached its present position at 6.5 ka BP, sediment infilling of the drowned estuary took 4–5 kyr (Hori *et al.* 2002; Xie *et al.* 2009). Once infilled some 2 kyr ago, the Changjiang sediment began to escape from the estuary on a large scale. One part of this sediment was deposited in the subaqueous delta, which today occupies an area of about 10^4 km^2 ; the other was transported southwards by shelf

currents. This observation implies that a critical level of river discharge exists below which delta growth does not occur. At the present stage, the critical level is between 180 and $300 \times 10^6 \text{ t a}^{-1}$ (Gao 2007). It furthermore implies that, under natural conditions, initial delta growth is rapid, but that the growth rate subsequently decreases until the growth limit is reached. Owing to the combined effects of natural processes and human activities, the growth rate of the delta has reduced in recent years, or has even come to an end (Gao *et al.* 2011; Y. H. Wang *et al.* 2013).

The modern Yellow River delta has a short but complex history (Xue 1993; Yu 2002). During the late Quaternary, especially over the last 150 kyr, this river brought a large quantity of sediment towards the sea, forming a vast coastal plain (Ren 2006). However, in northern China, it discharged different courses over the Holocene period (Chen *et al.* 2012). The Yellow River, in northern China, discharged alternatively into the Bohai Sea and the southern Yellow Sea during the Holocene. A large supply of sediments (i.e. 10^9 t a^{-1} , before the 1980s) caused the rapid formation of a delta immediately in the front of the river mouth. In the period from AD 1128 to AD 1855, the river discharged into the southern Yellow Sea, resulting in the formation of a large delta; since 1855, a delta consisting of six lobes and covering an area of 5500 km^2 of land has been formed (Shi *et al.* 2003). Before 1855, it discharged into the southern Yellow Sea on the Jiangsu coast. The Yellow River delta thus merely represents deposition over the last one and half centuries. It occupies an area of some 5600 km^2 , with a rate of shoreline advancement of around 10^2 m a^{-1} . Because of the rapid siltation in the channel and near the river mouth, the river frequently changed its route to reach the sea. In this way a number of lobes were formed, the shoreline of abandoned lobes being rapidly eroded (Chu *et al.* 2006).

The abandoned delta of the Yellow River located along the northern Jiangsu coast formed in the period from AD 1128 to AD 1855. In the course of this 727 years, the shoreline advanced by 50–60 km (Gao 2009a and the literature cited therein). At present, the abandoned Yellow River delta is eroding and provides the central Jiangsu coast with a certain quantity of fine-grained sediment.

Tidal flats

Tidal flats are distributed widely over the region, especially along the Jiangsu coast (SW Yellow Sea), the Shanghai and Zhejiang coasts, and the western Korean coast. This is consistent with the conditions of abundant fine-grained sediment supply and tidal dominance of the region (Gao

Table 3. Spatial distribution patterns of the major Holocene deposits

Sedimentary system	Spatial distribution pattern			Characteristics and architecture	Thickness of deposits	References
	Pattern	Area	Water depth			
Changjiang River delta	Typical funnel-shaped tide-dominated delta with three active elongated isolated river-mouth sandbars	c. 52 000 km ² (subaerial: 23 000 km ² ; subaqueous: 29 000 km ²)	c. 0–60 m	Thick deltaic deposits composed of tidal sand ridges, prodelta, delta-front, tidal-flats and surface soil deposits. Delta-front deposits: dark-grey silty to fine sand, and thickly interlaminated to thinly interbedded sand and mud. Sand mud couplets and bidirectional cross-lamination. Delta plain: upwards-fining succession and three subfacies: subtidal to lower tidal flat, upper intertidal flat and surface soil	c. 30 m (modern river-mouth area); c. 60–90 m (incised valley); >60 m with >80 m in incised valley	Li & Li (1983); Chen (1986); Li (1986); Orton & Reading (1993); C. X. Li <i>et al.</i> (2000, 2002); Hori <i>et al.</i> (2001a, 2002); Saito <i>et al.</i> (2001)
Yellow River delta	Elongated birdfoot-shaped wave-dominated delta, with a number of lobes	5500 km ² (since AD 1855)	–	Thin Holocene deltaic deposits with typical overall topset-foreset-bottomset configuration; a steep longitudinal profile in its lower reaches	c. 20–30 m	Saito <i>et al.</i> (2001); Shi <i>et al.</i> (2003)
The abandoned old Yellow River delta	Double clinoform mud wedge with a subaerial –subaqueous delta couplet	Subaerial: 7160 km ²	–	Large-scale clinoform with sewards-dipping lower angled (<0.3°) internal reflectors; a wide, gently inclined topset and a relatively narrow, steeply sloping foreset, stretching sewards about 160 km away from the shoreline	c. 4–16 m with a maximum of 20 m	Zhang (1984); Ren (1992); J. P. Liu <i>et al.</i> (2007); Liu <i>et al.</i> (2013)
Hangzhou Bay estuarine deposit	Funnel-shaped incised-valley fill	8500 km ²	c. 8–10 m	270 km long, 100 km wide at the estuary mouth; from bottom to top, the incised valley successions can be grouped into four sedimentary facies: river channel, floodplain estuary, estuary shallow marine and estuary sand bar	c. 20–60 m, average 26.5 m, valley up to 120 m	Lin <i>et al.</i> (2005); Xie <i>et al.</i> (2009)
Tidal flats on the Jiangsu coast	Typically c. 5–10 km wide with a significant zonation of salt marsh, mud flat, mixed	>5500 km ²	<5 m	667.5 km long, average bed slope 0.2%, silty sand–mud couplets with horizontal parallel bedding in mixed sand–mud flat and ripples,	c. 30 m	Zhu & Xu (1982); Ren <i>et al.</i> (1984); Zhang (1984); Ren (1986); Zhu <i>et al.</i> (1986, 1998); Yang <i>et al.</i>

Jiangsu Radial tidal ridges	sand-mud flat and sand flats c. 22 470 km ²	c. 0–30 m	small cross-bedding in sand flats; fining-upwards sequence Individual sand ridge 10–>100 km long, c. 10–15 km wide, furrows c. 10–30 m depth with a maximum of 48 m; flat-topped, comprises estuarine, tidal flat and shoreface deposits	c. 30 m	(2002); Gao (2009a); Y. Wang <i>et al.</i> (2012) Z. X. Liu <i>et al.</i> (1989, 1998, 2007); Zhu & An (1993); Y. Wang <i>et al.</i> (1999, 2012); Li <i>et al.</i> (2001)
Palaeo-tidal ridges on the East China Sea coast	Moribund sand ridges	c. 45–115 m	c. 60–110 m	Asymmetric transverse sections, with steep slopes facing SSW; orientation WNW–ESE, c. 10–60 km long with a maximum of 120 km, c. 8–14 km wide, c. 5–20 m high, average ridge spacing of c. 8–14 km; a complicated multi-layer architecture that reflects repeated accumulation–erosion–accumulation cycles	Up to 26 m (crest) Yang & Sun (1988); Z. X. Liu <i>et al.</i> (1998, 2000, 2003, 2007); Saito <i>et al.</i> (1998)
Tidal ridges off the South Korean coast	Moribund linear sand ridges on the mid-shelf, modern ridges on the inner shelf	37 000 km ²	c. 10–50 m, c. 50–90 m	Symmetric transverse profile, c. 30–200 km long, c. 3–13 wide, c. 13–25 m in height, covered by large bedforms (dunes) with wavelengths of c. 200–500 m; a thin surface recently reworked sand sheets of <5 m, and a thick transgressive sand ridge deposits of up to 20 m acoustically oblique or prograding clinoforms; composed of sand, sand–mud mixed and mud facies	10 ~ 25 m Park & Lee (1994); Liu <i>et al.</i> (1998); Jin & Chough (2002); Park <i>et al.</i> (2003, 2006)
Tidal ridges in the Bohai Sea	Six active, nearly paralleled finger-shaped sand ridges	c. 4000 km ²	c. 10–36 m	c. 8.7–43 km long, c. 6–20 m high; ridge spacing c. 8.3–16 m; multiple micro-geomorphic features comprise very large, large and medium subaqueous dunes, sand veneers and ribbons, scour furrows and comet-tail marks	c. 8–25 m with a maximum of 26 m Liu <i>et al.</i> (1994, 1998); Marsset <i>et al.</i> (1996); Liu & Xia (2004)
Yangtze Shoal	An active offshore tidal sand sheet; palaeo-Yangtze submarine delta	c. 30 000 km ²	c. 25–55 m	270 km-wide, 200 km-long subaqueous dune fields, c. 20 000 km ² . Medium- and small-sized bedforms: crestline spacing of c. 2.3–13.6 m and	8 ~ 25 m Liu (1997); Liu <i>et al.</i> (1998)

(Continued)

Table 3. *Continued*

Sedimentary system	Spatial distribution pattern			Characteristics and architecture	Thickness of deposits	References
	Pattern	Area	Water depth			
Yellow River distal mud	Complex sigmoidal-oblique clinoform	–	25–40 m	height of c. 0.20–0.97 m. Large and very large bedforms: crest-line spacing of c. 70–1265 m, heights of c. 0.5–2.6 m Lowermost (c. 2–3 m): retrogradational-aggradational stacking pattern with subhorizontal internal reflectors; Middle parts (c. 35 m): a prograding reflection pattern with mostly seawards-stepping reflectors separated by several erosive surfaces; Uppermost (maximum 18 m): an aggradational reflection pattern with sub-parallel reflectors	15–40 m	Liu <i>et al.</i> (2004); J. Liu <i>et al.</i> (2007)
Changjiang distal mud	Subaqueous mud wedge thins offshore and southwards	–	20 ~ 70 m	Nearly 800 km long, along the inner shelf (c. 100 m isobaths) from the Yangtze mouth to Taiwan Strait, across shelf distance <100 km	c. 20–40 m	J. P. Liu <i>et al.</i> (2006, 2007); Xu <i>et al.</i> (2009)
Huskan Mud Belt in the SE Yellow Sea	Southwards-prograding clinoforms	c. 8000 km ²	c. 10–50 m	2050 km wide, 200 km long; elongated morphology; overlies large-scale dunes	c. 10–20 m with maximum 60 m	Park & Yoo (1988); Park <i>et al.</i> (1999); Jin & Chough (1998); Chough <i>et al.</i> (2002, 2004)
Isolated mud patch in the central Yellow Sea	A relict generally SE-prograding subaqueous mud wedge	–	40–80 m	Rhythmic-stratified, interbedded sand and mud; subunits are parallel to sub-parallel or clinoformal with a sheet or wedge geometry	c. 10–40 m	Jin <i>et al.</i> (2002); Chough <i>et al.</i> (2004)

Note: ‘–’ denotes ‘lack of information’.

Table 4. Sedimentary characteristics of the major Holocene sedimentary systems over the region

Systems	Sedimentary characteristics			References
	Facies	Sedimentary structure	Sediment type	
Changjiang delta	Prodelta; delta front; subtidal to lower intertidal flat; upper intertidal flat; surface soil	Gradational contact with small-scale cut-and-fill structures; ripple and parallel laminations; thickly interlaminated to thinly interbedded dark-grey sand and mud; bidirectional ripple laminations; abundant plant rootlets and snail shells	Dark-grey silty clay; dark-grey silty to fine sand and sand-mud couplets sand and mud; coarse silt to very fine sand; dull reddish brown to brown clayey silt	Hori <i>et al.</i> (2001b)
Yellow River delta	Terrestrial/fluvial facies; estuary facies; delta front to prodelta facies; fluvial facies (natural levee and/or floodplain)	Parallel and ripple laminations; parallel lamination with sharp contact or lithological and colour; weathered foraminifer, shell fragments and pollen are found occasionally	Dark reddish brown to greyish brown clayey silt or alternation of clay and silt; dark brown to dark grey clay to very fine sand; greyish to yellowish brown silt to very fine sand	Saito <i>et al.</i> (2000)
The abandoned delta	Flood plain; prodelta; delta front	Weak lamination, oblique bedding with muddy intercalation; lamination; ripple and parallel laminations	Mud silt and sand; silt mud and mud silt; silt mud and mud silt	Yuan & Chen (1984)
Hangzhou Bay estuarine deposit	Vertical sequence: palaeo-estuary; shallow marine; estuary	Silt lens, flowing mucky and parallel laminations; silt lens	Greyish brown mud silt; fine silty sand	Wang <i>et al.</i> (2006); Lin (1997)
Tidal flat on the Jiangsu coast	Silt flat; mud and sand flat; salt-mash flat; marshland flat	Cross-bedding and graded bedding; current bedding, flaser bedding biological perturbation structure; horizontally laminated bed, root hole, fauna hole; flat bedding, plant root point and worm hole	Silt or fine sand; silt clay or silt; silt; clay silt or silt clay	Zhu <i>et al.</i> (1986)
Jiangsu radial tidal ridges	Basement; coast facies; tidal sand facies; littoral tidal-flat facies	Pedogenesis features; shell-sand lenses with low-angle cross-bedding, peat layers; flaser bedding, bidirectional cross-bedding and graded bedding; small cross-bedding, flaser and wavy bedding, abundant foraminiferal tests	Stiff mud; sandy mud; sand, silt-sand and mud of a grey colour; silt and clayey silt	Li <i>et al.</i> (2001)
Palaeo-tidal ridges on the East China Sea coast	Floodplain; estuary; shallow marine	Parallel and ripple laminations, discordant contact with underlying stratum; discordant contact with erosion surface; cross-bedding	Silt and mud silt; fine sand	Yang (2002)
Palaeo- and modern tidal ridges off the South Korean coast	Tidal flat and estuarine; shoreface to inner shelf; nearshore	Remnant laminae of silt-clay couplets with intense bioturbation; shell fragments and some gravels; low-angle cross-bedding	Sandy mud; sand; fine sand	Lee & Yoon (1997); Park <i>et al.</i> (2006)

(Continued)

Table 4. *Continued*

Systems	Sedimentary characteristics			References
	Facies	Sedimentary structure	Sediment type	
Tidal ridges in the Bohai Sea	Nearshore; shallow marine; tidal sand sheet	Discordant contact with underlying stratum, shell fragments, plant residue; laminated clay layers	Clay silt and silt clay with sand gravel; silt clay; fine sand	S. F. Liu <i>et al.</i> (2008)
Yangtze Shoal	Shallow marine	Tidal rhythms, wavy and herringbone cross-beddings	Sand	Ye <i>et al.</i> (2004); Liu (1997)
Yellow River distal mud	Salt marsh and coastal plain; subtidal nearshore; deepening shelf; deep shelf	Sandy lenses and clayey flasers, moderate bioturbation with plant fragments; lenticular bedding with shell fragments; clayey silt intercalated with sand layers or lenticular beds, molluscan shell fragments occur sporadically; sandy laminations found occasionally, slight bioturbation with shell fragments	Dark grey to greyish silty clay to silt; silt to sandy silt; dark grey clayey silt; dark greenish grey to dark grey clayey silt	J. P. Liu <i>et al.</i> (2007)
Changjiang delta mud	Nearshore; shallow sea shelf	Stacked fining-upwards parasequences of transgression	Light grey sandy silt; light grey and taupe clayey silt and clay	Xiao <i>et al.</i> (2006)
Huskan Mud Belt in the SE Yellow Sea	Tidal sand ridges/tidal flat	Parallel-laminated structures, massive bedding and worm hole; homogeneous mud with some shells and shell fragments	Silt and clay; silt sand and sand	Park <i>et al.</i> (2000)
Isolated mud patch in the central Yellow Sea	Tidal shallow marine; transition facies; shallow marine	Discontinuous current bedding with shell fragments, rare plant root point and rare worm hole; cross-bedding with rare shell fragments and worm hole; stratification, moderate bioturbation, block structure and shell fragments	Clay silt; clay silt; clay silt	L. B. Wang <i>et al.</i> (2009)

Note: ‘–’ denotes ‘lack of information’.

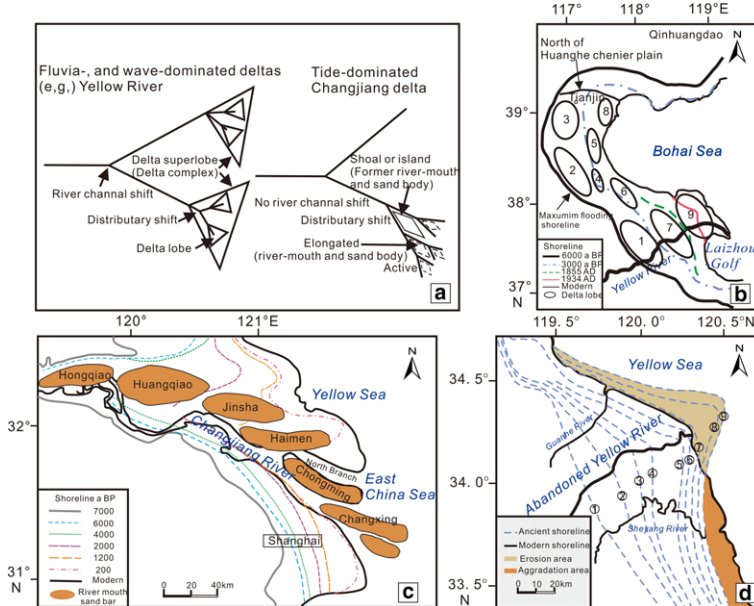


Fig. 6. Characteristics of the river deltas in the study area: (a) a summary of the general characteristics of the Yellow River and Changjiang River deltas (after Hori *et al.* 2002); (b) the Yellow River delta (age of the various delta lobes: (1) 6–5 ka BP; (2) 5–4.5 ka BP; (3) 4.5–3.4 ka BP; (4) 3.4–3 ka BP; (5) 3 ka BP–602 BC; (6) 602 BC–AD 11; (7) AD 11–AD1048; (8) AD 1048–AD 1128; (9) AD 1855–present (after Xue 1993; Saito *et al.* 2000, 2001); (c) the estuarine sand-body ages in the Changjiang delta at: Hongqiao, 7.5–6 ka BP; Huangqiao, 6.5–4 ka BP; Jinsha, 4.5–2 ka BP; Haimen, 2.5–1.2 ka BP; Chongming, 1700–200 years BP; Changxing, 700 years BP (after Li *et al.* 1979; Li & Li 1983; Xu *et al.* 1987); and (d) the abandoned (old) Yellow River delta (after Ye 1986; L. Zhang *et al.* 2014; the numbers ①–⑨ indicate shorelines in the years of AD 1194, 1578, 1591, 1700, 1747, 1776, 1803, 1810 and 1855, respectively).

2009a). In areas of small river inputs, in contrast, tidal flats are either located in well-sheltered embayments or in estuarine bay head areas along the coastline of Europe (e.g. Evans 1965).

The tidal flats on the Jiangsu coast are on the largest scale in the region, where the intertidal zone occupies an area of more than 5500 km² (Ren 1986). Sediment distribution is controlled here by tidal action. Sediment supplied by the Changjiang and Yellow rivers consists of fine-grained sand, silt and clay. The upper parts of the flat system experiences slow changes in water level with weak currents; thus, only muddy material can reach these parts. Over the middle–upper intertidal zone, the tidal current is weak at neap tides, but strong at spring tides. Mud is deposited at neap tide and sandy material at spring tide, thereby forming typical heterolithic tidal bedding. The lower intertidal zone is associated with bedload transport. Therefore, from upper to lower tidal flats, the sediment zonation is characterized by thinly laminated muds, alternating mud and sand layers (i.e. tidal laminae), and cross-bedded sands, respectively. For the region, these zones are referred to as

mudflat, mixed mud–sand flat and sand flat, respectively (Zhu & Xu 1982; Zhang 1992). During storms, the combined storm surge and tides enable seawater to reach the supratidal zone; in this case, accretion takes place on the uppermost part, but erosion occurs on the lower intertidal zone (Ren *et al.* 1985).

Because of the sustained sediment supply, the shoreline has continued to advance seawards. Even after the Yellow River switched to its north-easterly route, erosion of the abandoned delta provides the sediment source that resulted in accretion along the central Jiangsu coast at a rate of 50–150 m a⁻¹. At the same time, the morphology of the tidal flat was maintained by natural processes (Liu *et al.* 2011). In addition to this general trend, the cross-shore tidal-flat profile may be influenced by the presence of tidal creeks (Zhang 1992; Y. P. Wang *et al.* 1999), which modify the time–velocity asymmetry, while also influencing salt marsh growth (Y. P. Wang *et al.* 2012; Gao *et al.* 2014), thereby causing localized changes in the erosion–accretion pattern. The expansion of *Spartina* (an artificially introduced species) had significant

effects (Y. P. Wang *et al.* 2012; Gao *et al.* 2014). The original deposition patterns have been changed (Fig. 7): in response to the expansion of *Spartina*, intensified accretion took place on the upper tidal flat, thereby causing rapid shoreline advancement, and, at the same time, the lower tidal flat zone was narrowed, sometimes associated with the formation of salt-marsh cliffs at the marsh–mudflat boundary (Zhao *et al.* 2014).

With the reduction in sediment supply, coastal erosion has been intensified on the northern Jiangsu coast, to the immediate south of the abandoned Yellow River delta. This represents a natural response to the cut-off of sediment supply. When coastal recession occurs, the profile shape of tidal flats cannot be maintained: the lower flat is initially eroded, enhancing the average slope of the entire intertidal zone, followed by erosion of the entire tidal-flat area. This process eventually results in the formation of eroding cliffs along the salt-marsh

edge (Zhao *et al.* 2014). In the middle Holocene, a series of cheniers were formed on the Jiangsu coastal plain, now 50–60 km away from the sea dyke (Wang & Ke 1989). These represent the final product of tidal-flat erosion at that time.

The sedimentary record of the tidal flat has a high temporal resolution, although the preservation potential varies between the mudflat, mixed flat and sand flat (Gao 2009b). For example, on the central part of the Jiangsu coast, the sediment supply from the Yellow River from AD 1128 to AD 1855 resulted in rapid evolution of the tidal-flat system (see above). The shoreline advanced at a rate of 10^1 m a $^{-1}$. Even after the northwards shift of the Yellow River mouth to the Bohai Sea, erosion of the old delta continued to supply fine-grained sediment (Yu *et al.* 2014). Thus, a vast coastal plain formed with an up to 20 m-thick Holocene tidal-flat deposit. The high resolution and continuity of the tidal-flat deposit make it an ideal sedimentary

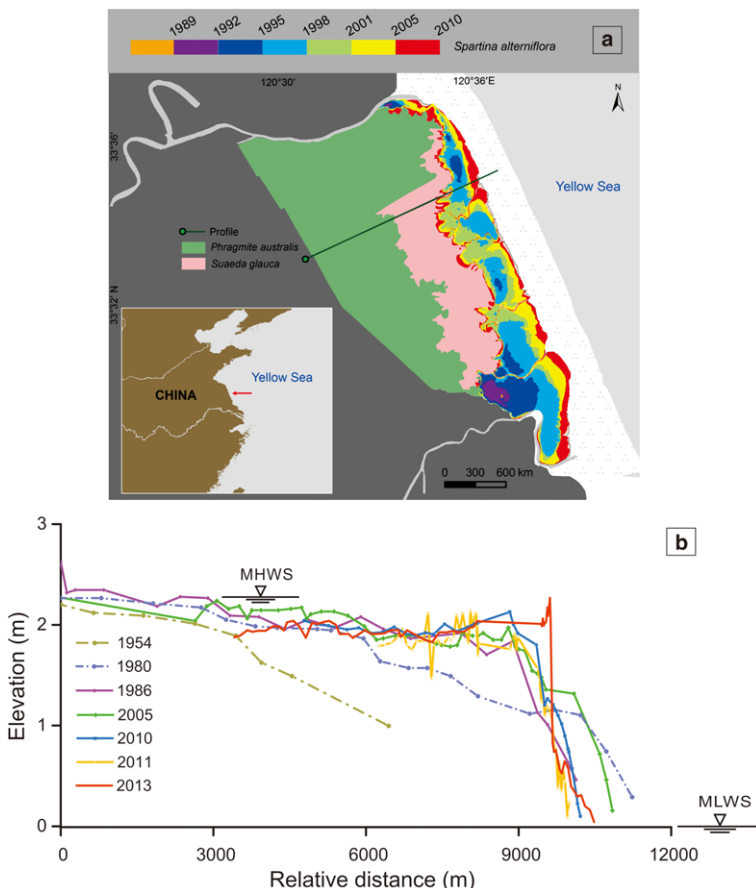


Fig. 7. Tidal-flat morphology on the central Jiangsu coast, before and after colonization by *Spartina alterniflora*: (a) location of the coastal profile; and (b) coastal profile changes between 1954 and 2013.

record for sea-level, climate, environmental and ecosystem change studies. In particular, the fine-grained materials, including both inorganic materials and organic matter, contain extensive information on past environmental changes.

On the central Jiangsu coast, the shoreline dynamics during the last 6.5 kyr is still poorly understood. From the middle Holocene (*c.* 6.5 ka BP) to the Song Dynasty in AD 1128, the shoreline advanced slowly towards the sea (*i.e.* 10 km over 5 kyr). However, during the subsequent 727 years, when the Yellow River discharged into the SW Yellow Sea, the shoreline advanced by 50–60 km (Gao 2009a and the citations therein). Thus, the rate of shoreline change for these two periods differs by an order of magnitude. At present, the central Jiangsu coast continues to accrete in response to material supply from the eroding former Yellow River delta (Yu *et al.* 2014) and offshore radial sand ridges (Fu & Zhu 1986), but the relative importance of these two sources is unknown. If the offshore areas represent a major sediment source, then it needs to be explained why, during the earlier periods, the shoreline did not prograde at the same rate as today. To answer this question, the shoreline evolution before AD 1127 can be modelled to gain some insight into the changing sediment dynamic conditions associated with the radial tidal ridges, in terms of seabed reworking and landwards transport of fine-grained sediment. Furthermore, the abandoned Yellow River delta and the central Jiangsu coast can be treated as a small-scale source–sink system, for which *in situ* measurements and numerical simulation can be carried out to reveal the evolution pattern of the sedimentary system since the Song Dynasty. Figure 8 shows the shoreline changes since the middle Holocene; in order to explain such a complex changing pattern, the sediment budget in association with the Changjiang and (old) Yellow rivers and the reworking of offshore pre-Holocene strata should be evaluated.

The tidal flats along the coast to the south of the Changjiang Estuary and on the eastern Yellow Sea coast (*i.e.* the South and North Korean coasts), which are mainly confined to coastal embayment, have similarities to the Jiangsu counterparts. They are also characterized by zonation and fining-upwards sequences. However, because in these places the supply of fine-grained sediment is mainly provided by rivers not directly discharging into the deposition area, the systems are characterized by a lack of sand. As a result, the sand flat in the lower intertidal zone is narrow, or even absent. For instance, the Zhejiang–Fujian coast was originally a rocky coast that was gradually converted into an intertidal flat by the long-distance import of the Changjiang River (Li & Wang 1991). As a result, a narrow coastal plain developed. Because

the sediment supply consists only of mud, the zonation of the tidal flats differs from that of the Jiangsu coast. Nevertheless, a general fining-upwards trend is still present. In addition, the width of the intertidal zone is smaller than at Jiangsu.

Tidal ridges and other sandy deposits

Being a tide-dominated region, tidal ridges are well developed. These include the Jiangsu radial tidal ridges, the palaeo-tidal ridges on the East China Sea shelf, the Yellow Sea tidal ridges off the North Korean coast and the tidal ridges in the eastern Bohai Sea (Fig. 9). The coastlines of the ridges are parallel or sub-parallel, aligned to the main tidal flow direction and attain lengths of 100 km, their spacing ranging from 1 to 10 km and inter-ridge channel depths reaching 10–30 m. Typical examples from other regions are the parallel ridge systems of the North Sea in Europe (Berné *et al.* 1994; Trentesaux *et al.* 1999; Deleu *et al.* 2004).

On the Jiangsu coast, China, a large-scale, radially arranged tidal-ridge system is present (Y. Wang *et al.* 2012; Xing *et al.* 2012) (Fig. 9a). Here the tidal current is very strong, reaching up to 3 m s^{-1} . The sediment of the ridges consists mainly of fine to very fine sands derived from the underlying pre-Holocene strata (Li *et al.* 2001). The 70+ ridges cover an area of around $25 \times 10^3 \text{ km}^2$. Compared with the North Sea counterpart (Huthnance 1982a, b), the local ridges are more mobile (Gao & Collins 2014). For example, an inter-ridge channel was recorded to have formed within 3 years, the water depth increasing from 3 to 11 m (Zhang & Chen 1992). System response is evidently much shorter than in the North Sea. In addition, the crests of the North Sea ridges are not exposed at low tide, whereas the landwards transport of fine-grained sediment along the Jiangsu coast causes the shorewards parts of the ridges to merge with the intertidal flats. These differences result from the fact that the grain size is relatively small and the tidal currents are relatively strong on the Jiangsu coast compared with the North Sea.

The palaeo-tidal ridges on the East China Sea shelf (Fig. 9b) are located in water depths of 40–60 m. Because these were thought to be immobile under the present-day tidal regime, they were referred to as ‘moribund’ ridges. Numerical modelling has indicated that, during the early periods of the Holocene when sea level was lower than present day, the tidal currents were, indeed, much stronger (Uehara *et al.* 2002). The pre-Holocene deposits in this region are composed of sediments rich in mud. It was thus postulated that the ridges were formed in the course of seabed erosion, the sand being transported into the ridges, while the mud was carried away. When comparing the model

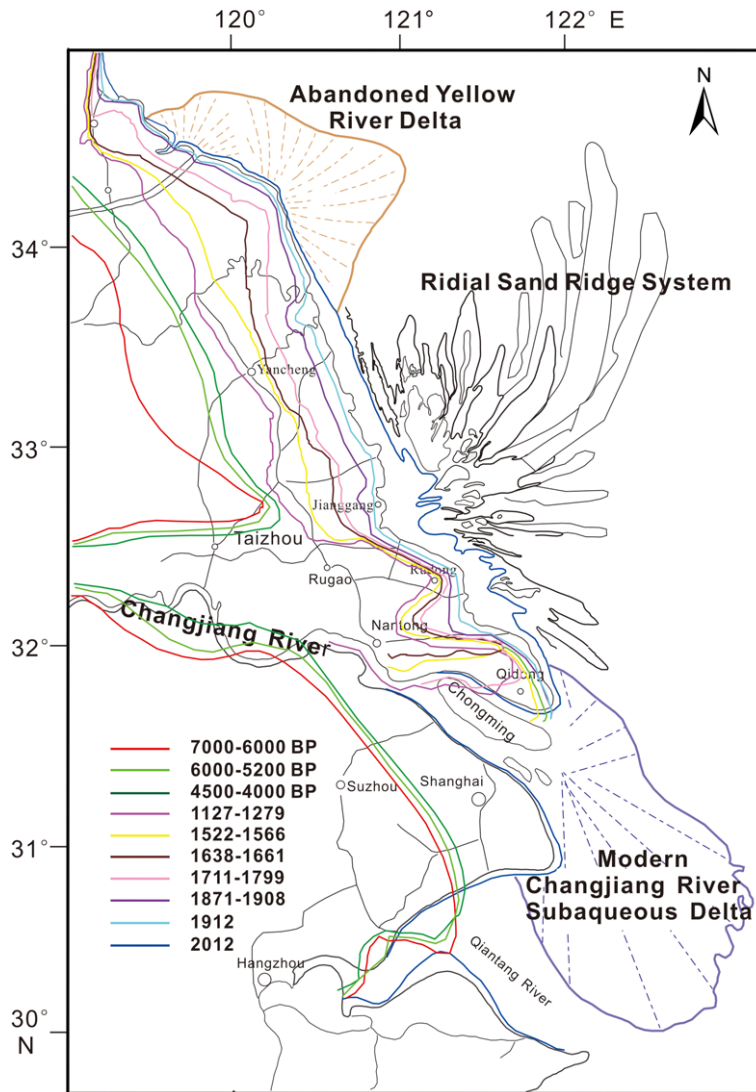


Fig. 8. Shoreline changes on the Jiangsu coast and sediment source–sink for the Holocene deposits (based on Zhu *et al.* 1996; X.X. Zhang *et al.* 2014).

output with the conditions for the tidal-ridge formation, as suggested by Liu *et al.* (1998), the areas suitable for tidal-ridge development at the various stages of sea-level rise during the early Holocene are highly consistent with the occurrence of the old ridges (Fig. 10). However, tidal cycle measurements show that, under the present conditions, the tidal current still exceeds the threshold of bedload motion: that is, the sediment here is mobile (Z. X. Liu *et al.* 2007). Further, seismic surveys and core analyses have indicated that the ridges are

migrating. Thus, active ridges may exist in deeper shelf waters, if the tidal current is sufficiently strong.

The tidal ridges in the eastern Bohai Sea (Fig. 9c) are also formed by the reworking of the underlying strata (Z. X. Liu *et al.* 2007). Here, the sedimentary materials were derived from seabed erosion of the NW Bohai Strait, where the tidal current is strong. At first, the seabed was eroded and the material transported into the Bohai Sea, where it later formed the base of the tidal ridges. At later stages, the channel in the Strait was further deepened by tidal

HOLOCENE SEDIMENTARY SYSTEMS

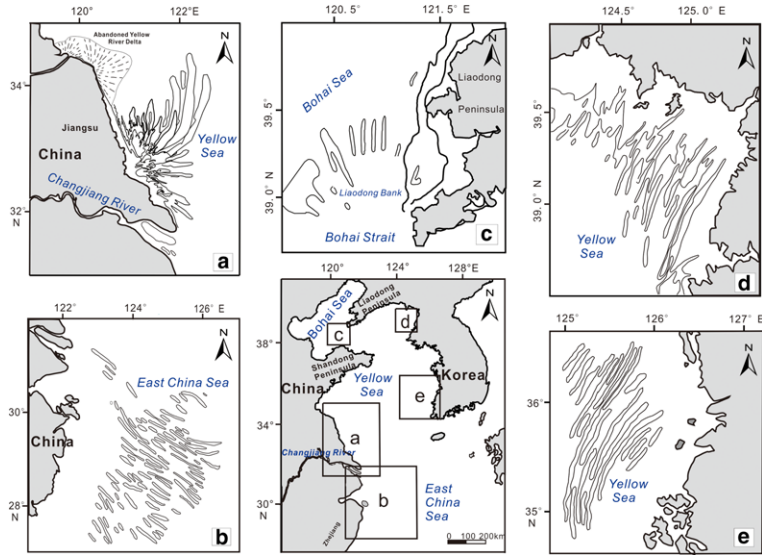


Fig. 9. Tidal-ridge systems of the region: (a) Jiangsu radial tidal ridges (from Li *et al.* 2001; Gao 2014); (b) palaeo-tidal ridges on the East China Sea shelf (from Z. X. Liu *et al.* 2007); (c) tidal ridges in the eastern Bohai Sea (from Liu 1997); (d) Yellow Sea tidal ridges off the North Korean coast (from Off 1963); and (e) Yellow Sea tidal ridges off the South Korean coast (from Park *et al.* 2006).

scouring, with the sediment being continuously transported into the tidal-ridge area. As verified by ^{14}C dating, the material at the surface is older than

that at the base; this is because the dates represent the timing of the biologically generated sediment, rather than the time of deposition (Scholl 1964).

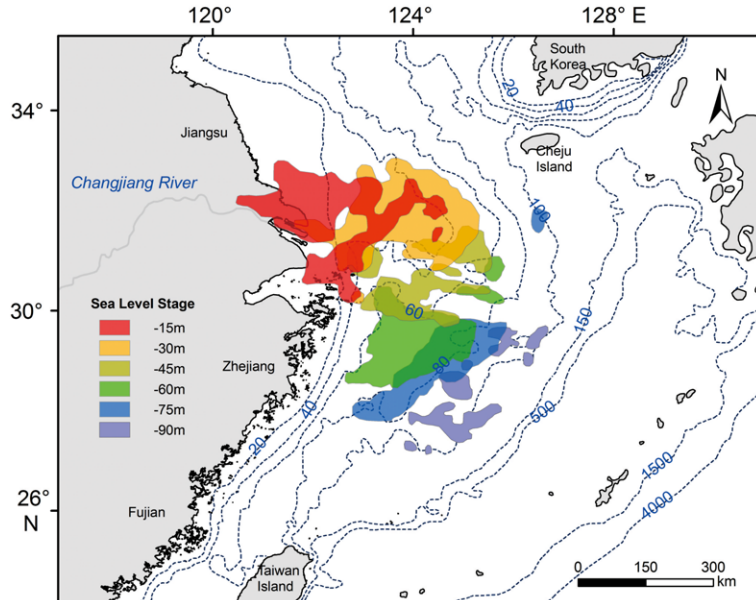


Fig. 10. Model output for the formation of the palaeo-tidal-ridge system on the East China Sea shelf (modified from Uehara *et al.* 2002; Uehara & Saito 2003).

The Yellow Sea tidal ridges off the Korean coast (Fig. 9d, e) follow the classical theory of linear sandbanks, based upon the North Sea studies (Huthnance 1982a, b). Over the tidal-ridge field off the North Korean coast, the tidal-current speed reaches 1 m s^{-1} and the sediment is derived from the reworking of pre-Holocene strata (Off 1963). The ridges off the South Korean coast consist of two groups: the mid-shelf ridges (water depth of 50–90 m) and the inner-shelf ridges (water depth of <30 m). The former group resulted from the reworking of the pre-Holocene strata during the post-glacial transgression, whilst the shallow-water group is a product of modern tidal processes (Park *et al.* 2006).

If the condition of rectilinear tidal currents is not satisfied, then tidal ridges cannot develop. The critical value of a tidal ellipse ratio (of the lateral component to the longitudinal component of the tidal current) was shown to be 0.4; only at ratios below this value can tidal ridges be formed (Liu 1997). For rotatory currents, in contrast, tidal sand sheets will be formed. For example, the Yangtze Shoal off the Changjiang River mouth is a tidal sand sheet (Liu 1997). Similar to the tidal ridges off the central Jiangsu coast, the sediment composing the sand sheet has also been derived from the underlying pre-Holocene relict deposit. However, it differs from the tidal ridges in that the reworking here is weaker: the sand sheet serves as an armour layer, which now protects the underlying strata from further erosion.

Coastal and shelf mud deposits

The study area is characterized by numerous, widely distributed mud deposits (Fig. 2). In terms of sediment provenance and the transport processes involved, these can be divided into distal mud deposits associated with large rivers, coastal mud belts and isolated mud patches on the shelf.

The distal mud deposits (or remotely distributed clinoform deltas) associated with the Yellow and Changjiang rivers are today well known. The distal mud deposit of the Yellow River is located to the NE of the Shandong Peninsula, up to 600 km away from the river mouth in the western Bohai Sea (Yoo *et al.* 2002; Liu *et al.* 2004, 2006; J. Liu *et al.* 2007); the distal mud deposit of the Changjiang River is located on the inner shelf of the Zhejiang–Fujian coast, up to 800 km away from the river mouth.

Both the distal muds associated with the Changjiang and Yellow rivers are characterized by clinoforms. There are basically two types of clinoforms: convergent and parallel clinoforms (Gao & Collins 2014). The Yellow River distal mud has well-developed convergence and parallel

clinoforms, which represent early and later evolutionary stages of distal mud deposition, respectively. At first, the depocentre (i.e. the location with the highest deposition rate) was coincident with the maximum suspended sediment concentration, since the settling flux is proportional to the concentration. As a result, the central part of the mud deposit had the highest elevation, and the sedimentary layers thin from there to the distal edge. Subsequently, as the slope towards the edge increased, the bottom layer moved outwards, under the influence of gravity, to form parallel clinoforms. At the same time, the highest part of the deposit experienced increased current speeds (in response to a reduction in water depth). This interpretation implies that the parallel clinoforms serve as evidence of the effect of sediment gravity flow (Gao & Collins 2014). At the distal mud of the Yellow River, the top of the deposit has a water depth of around 30 m; the two types of clinoforms have been detected on shallow seismic records (Liu *et al.* 2004).

The distal mud of the Changjiang also shows the presence of clinoforms (J. P. Liu *et al.* 2007). However, compared with its Yellow River counterpart, the parallel clinoforms are not yet well developed. As revealed on shallow seismic records, the clinoforms associated with this mud deposit are dominated by the convergence type, only in some places have parallel ones begun to grow. As in the case of the Yellow River counterpart, the elevation of the Changjiang mud deposit is around 30 m. Thus, compared with the Yellow River system, this deposit is less mature in terms of the evolutionary stages. In fact, in southern China, the distal mud of the Pearl River is at an even younger stage: although the distal mud occupies a large area (i.e. $>8000 \text{ km}^2$ on the inner shelf of the northern South China Sea, some 600 km away from the river mouth), the mud layer is still rather thin and, hence, lacks clinoform development (Liu *et al.* 2014). The seabed elevation here is located more than 40 m below the sea surface.

The differences in the timing and duration of the three distal mud deposits have been interpreted to be the result of estuarine sediment-infilling processes (Liu *et al.* 2014). The Yellow River did not have a large estuary when sea level reached the high level at 7 ka BP and the sediment discharge was large. Hence, the material discharged by the river was supplied to the distal mud deposit from the start, resulting in continuous accumulation. In the case of the Changjiang, the estuary at 7 ka BP was large and, before infilling was complete, little sediment escaped to the open shelf. It took more than 4 kyr for the estuary to become completely infilled. Therefore, the supply of muddy sediment to the distal mud repository only began about

2 kyr ago. Prior to this, the distal mud was composed of sediment reworked from pre-Holocene shelf deposits. The Pearl River has an even larger estuary and the river discharge is relatively low. Hence, the infilling of the estuary is still ongoing today and only very recently (i.e. some 100 years ago) did the Pearl River sediment begin to escape from the estuary to reach the distal mud area (Liu *et al.* 2014). Hence, the three distal mud systems may be viewed as reflecting different stages of evolution: the Yellow River mud represents a mature stage, the Changjiang River mud a developing stage and the Pearl River mud an early stage (Fig. 11).

It should be noted that the Changjiang distal mud (i.e. the Zhejiang–Fujian shelf mud) may not entirely be composed of modern Changjiang sediments. At present, the Changjiang is, indeed, the source, from where it is transported southwards by shelf currents (J. P. Liu *et al.* 2006, 2007; K. H. Xu *et al.* 2009, 2012). However, borehole analyses (i.e. grain size and ^{14}C age determination) of the Zhejiang–Fujian mud area have revealed a significant 4 kyr hiatus in the sediment sequence (Liu

et al. 2006; Xu *et al.* 2011): below the upper, younger than 2 kyr layer, the strata are generally older than 6 kyr (Fig. 12). Similar patterns have been identified for Hangzhou Bay (X. Zhang *et al.* 2014) (see Fig. 12). In terms of the model, this would mean that the uppermost layer was deposited after the Changjiang Estuary had been infilled (see above). The lower part differs from the upper one in that it contains a relatively high sand content (Xiao *et al.* 2006), and the average deposition rate on the basis of ^{14}C dating is lower than the upper layer, indicating discontinuous sediment accumulation (Xu *et al.* 2012). These characteristics indicate that the sediment source changed since early Holocene times. The tidal-ridge systems on the East China Sea shelf may have served as a major sediment source for the formation of the lower layers. As described above, to form these ridges a large amount of fine-grained sediment would have to have been reworked (Z. X. Liu *et al.* 2007), stronger than present tidal currents providing the hydrodynamic forcing (Uehara *et al.* 2002), which resulted in landwards transport of the fine-grained

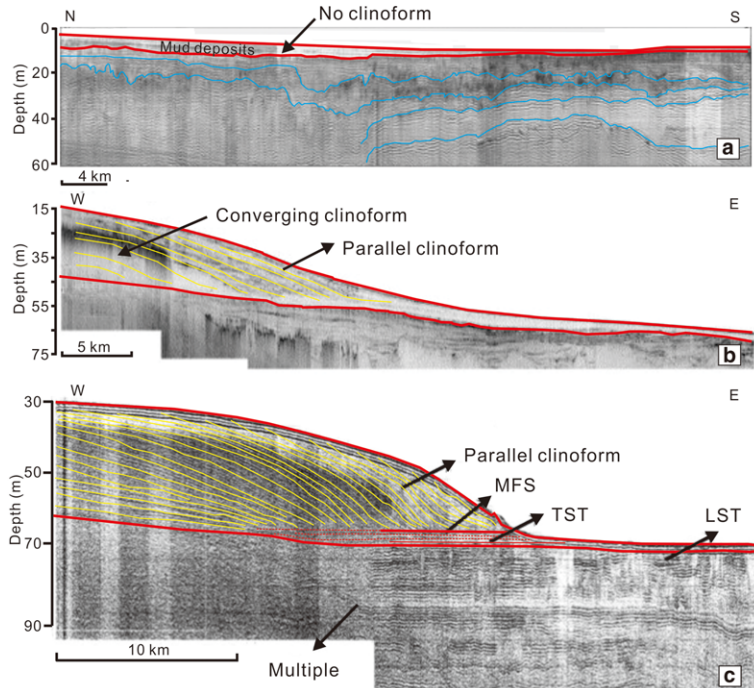


Fig. 11. Evolution stages of the distal mud deposits associated with large rivers: (a) early stage, represented by the situation on the northern shelf of the South China Sea, associated with the Pearl River (Liu *et al.* 2014); (b) developing stage, represented by the frontal part of the Yellow River distal mud and the Zhejiang–Fujian coastal mud associated with the Changjiang (Liu *et al.* 2006); and (c) mature stage, represented by the Yellow River distal mud in the eastern Bohai Strait (Liu *et al.* 2004). LST, lowstand systems tract; MFS, maximum flooding surface; TST, transgressive systems tract.

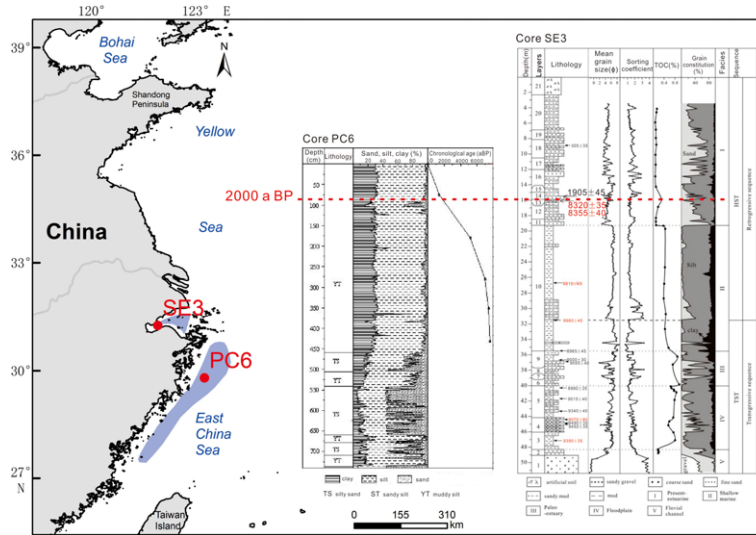


Fig. 12. Hypothesized source–sink characteristics of the Changjiang distal mud and the Holocene sequences of Hangzhou Bay (after Liu *et al.* 2006; Xiao *et al.* 2006; Xu *et al.* 2011; Zhang X *et al.* 2014). 2000 a BP = 2 ka BP.

material. This material was mixed with the inner-shelf sediment (and partly the river-derived sediment); as a result, the ^{14}C -derived sediment age would be older than the materials in the source area. This hypothesis can explain the sediment sequences shown in Figure 12, but further studies on sediment provenance and sediment-transport modelling are required to test this hypothesis.

The Holocene Hangzhou Bay estuarine incised valley fill has a thickness of up to 100 m (Lin *et al.* 2005). Of this sequence, the modern Changjiang sediments (supplied over the last 2 kyr) only occupy the uppermost 20 m (Yu *et al.* 2012; X. Zhang *et al.* 2014). Because before 2 ka BP not much Changjiang sediment reached Hangzhou Bay, the older sediments may also have had an offshore source, similar to the Zhejiang–Fujian shelf mud (see above). Hence, we propose the same hypothesis for the Hangzhou Bay mud deposits: the reworking of pre-Holocene strata and subsequent tidally induced transport were responsible for the formation of the thick mud deposits. Once again, this hypothesis should be tested by further investigations.

While large amounts of sediment are trapped on the inner shelf of the East China and Yellow seas, some material has been dispersed by shelf currents. Generally, the mud deposits formed in this way are associated with a low deposition rate and low temporal resolution. The mud deposit over the central Yellow Sea and to the south of Cheju Island in the southern Yellow Sea belongs to this category (Lim *et al.* 2007). Here, the tidal currents are weak (i.e.

below the threshold for the initiation of sediment movement). Fine-grained sediment from various sources (including reworked and modern-day river input) has accumulated in this region, together with biogenic particles (Gao & Jia 2003). The sediment was transported by shelf currents (Park *et al.* 2001) before finally settling to the bed. Vertical circulation may, in addition, contribute organic material and thereby enhance deposition. In this way, a 1–10 m-thick sediment layer formed in the course of the late Holocene. Because the water depth lies within the range of wave action (Graber *et al.* 1989), resuspension may occur under extreme conditions. A mechanism related to an upwelling or coupled upwelling–downwelling system has been proposed to explain the deposition patterns and the enhancement of the organic matter content (Fig. 13): particles generated by biological activity will be concentrated in the core area of the system; as a result, the accumulation rate may be enhanced, and the dissolved nutrient content may become higher than that of the surrounding waters owing to degeneration of the organic particles (Gao & Jia 2003).

Discussion

Process–product relationships for the Holocene deposits

As outlined above, the broad shelf and an abundant terrestrial sediment supply determined the spatial

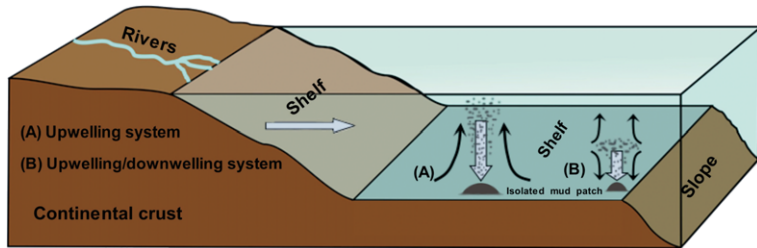


Fig. 13. Water-column processes for the formation of the isolated mud patches in the central Yellow Sea and to the south of Cheju Island (after Gao & Jia 2003; base diagram from Frank 2011).

distribution and temporal evolution of the various Holocene sedimentary systems in the region considered here. From the point of sediment dynamics, an understanding of the transport and accumulation processes will lead to a sound prediction

of the product (i.e. the Holocene deposits), while including the tidally dominated or combined tide–wave-dominated deposits, shelf-circulation-generated deposits and the deposits influenced by sediment gravity flows.

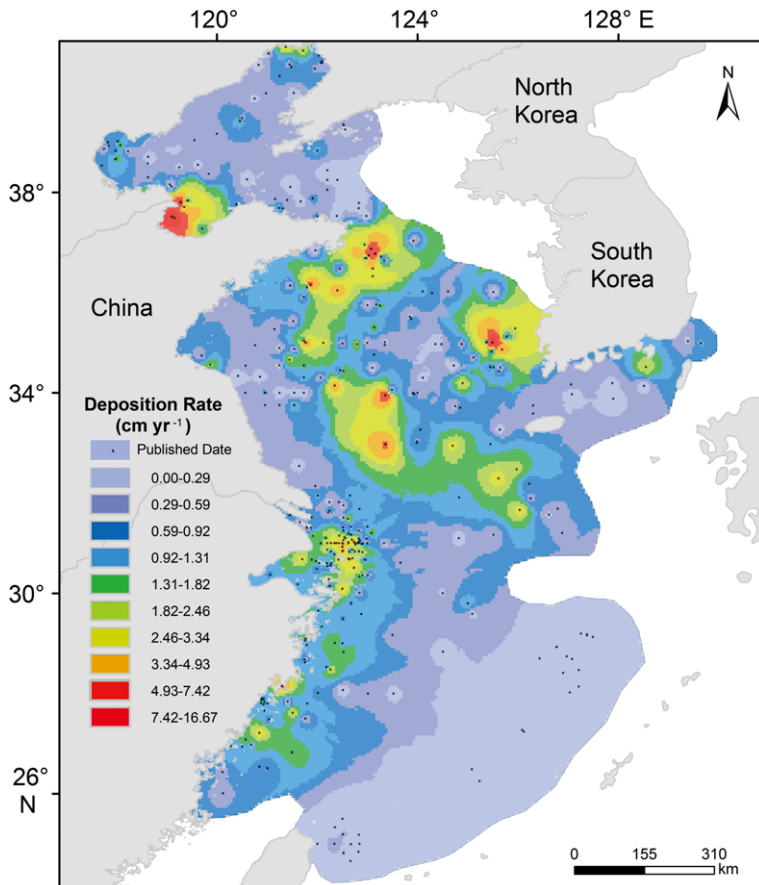


Fig. 14. Contemporary deposition rates of the region, as derived from ^{210}Pb and ^{137}Cs analysis (compiled on the basis of DeMaster *et al.* 1985; Alexander *et al.* 1991; Huh & Su 1999; F.Y. Li *et al.* 2002, 2006; Oguri *et al.* 2003; Lim *et al.* 2007).

Table 5. Temporal resolution, continuity and time coverage of the sedimentary records associated with the major Holocene deposits over the region

Sedimentary system	Starting time	Temporal resolution	Duration	Mechanisms/factors influencing continuity	References
Changjiang River delta	c. 8.5–6 ka BP	100 years	c. 6 ka–present	Progressive and lateral shift towards the SE	Li (1986); Chen & Stanley (1995); C. X. Li <i>et al.</i> (2000, 2002); Saito <i>et al.</i> (2001); Hori & Saito 2007; Hori <i>et al.</i> (2001b, 2002); Gao (2007)
Yellow River delta	c. 7–6 ka BP	100 years	LGM– c. AD 1128 c. AD 1855–present	Lateral channel avulsion and migration	Zhang (1984); Saito <i>et al.</i> (2001); Liu <i>et al.</i> (2004); Xue <i>et al.</i> (2004)
Abandoned Old Yellow River delta	AD 1128	10–100 years	c. AD 1128–AD 1855	Coastal erosion	Zhang (1984); Liu <i>et al.</i> (2013)
Hangzhou Bay estuarine deposit	LGM 2 ka	10 years	LGM– c. 6 ka c. 2 ka–now	Hydrodynamic disturbance and weak bioturbation	Feng <i>et al.</i> (1990); Lin <i>et al.</i> (2005)
Tidal flats on the Jiangsu coast	c. AD 1500	<1 year–1 day	c. AD 1500– present	Vertical mixing by bioturbation, storms and frequent migration of tidal creeks	Ren <i>et al.</i> (1984); Zhang (1984); X. Y. Liu <i>et al.</i> (2008); J. Wang <i>et al.</i> (2010); Li <i>et al.</i> (2011); Y. Wang <i>et al.</i> (2012)
Jiangsu radial tidal ridges	c. 7 ka BP	–	c. 2 ka to present	Shift of tidal channels; bed erosion during storm events	Zhang <i>et al.</i> (1998); Li <i>et al.</i> (2001); Z. X. Liu <i>et al.</i> (2007); Y. Wang <i>et al.</i> (2012)
Palaeo-tidal ridges on the East China Sea coast	c. 11–9 ka BP	–	c. 11–6 ka BP	Lateral sand ridge migration towards the SW, and new ridges continually replacing old ones	Uehara <i>et al.</i> (2002); Z. X. Liu <i>et al.</i> (2003, 2007)

Palaeo-tidal ridges off the South Korean coast	<i>c.</i> 14–9.5 ka BP	–	<i>c.</i> 14–< 8 ka BP	Lateral migration	Park & Lee (1994); Liu <i>et al.</i> (1998); Jin & Chough (2002); Park <i>et al.</i> (2003, 2006)
Modern tidal ridges off the South Korean coast	<i>c.</i> 7 ka BP	–	–	Lateral migration	Park <i>et al.</i> (2006)
Tidal ridges in the Bohai Sea Yangtze Shoal	8 ka BP <i>c.</i> 9–8 ka BP <i>c.</i> 14–10 ka BP	–	<i>c.</i> 8 ka BP–present	Material supply from the adjacent Bohai Strait Seabed erosion, bioturbation	Ren & Shi (1986); Xia <i>et al.</i> (1995); Liu <i>et al.</i> (1998) Chen (1986); Liu (1987); Qin <i>et al.</i> (1987); Jin (1992); Liu <i>et al.</i> (2004)
Yellow River distal mud	<i>c.</i> 11.6–9 ka BP	10–100 years	–	Water depth and sediment transport due to currents and gravity flows	Liu <i>et al.</i> (2002, 2004); J. Liu <i>et al.</i> (2007)
Changjiang distal mud	<i>c.</i> 7 ka	10 years	–	Water depth and sediment transport due to currents and gravity flows	J. P. Liu <i>et al.</i> (2006, 2007); Liu <i>et al.</i> (2010)
Huskan Mud Belt in the SE Yellow Sea	Since 8 ka BP	100 years	–	Intense bioturbation, seabed erosion	Chough <i>et al.</i> (2004); Lim <i>et al.</i> (2007)
Isolated mud patch in the central Yellow Sea	<i>c.</i> 9.5–7.5 ka BP	100 years	–	Intense bioturbation, seabed disturbance during storms	Milliman <i>et al.</i> (1987, 1989); Jin <i>et al.</i> (2002); Lim <i>et al.</i> (2007)

Note: ‘–’ denotes ‘lack of information’.

Although much effort has been expended to understand the sediment-transport patterns, the question of how these relate to the depositional characteristics of the Holocene sedimentary systems has received much less attention. In the first place, the magnitude of the deposition rate can be explained by sediment dynamic observations. Over the years, a large dataset has accumulated on the basis of ^{210}Pb and ^{137}Cs analyses, and a relatively good spatial coverage (Fig. 14). In the mud area of the central Yellow Sea, the deposition rate is of the order of 1 mm a^{-1} . This deposition rate must be seen in relation to a shelf-circulation velocity of 0.1 m s^{-1} , a suspended sediment concentration of 0.01 kg m^{-3} , a water depth of 50 m and net sediment-transport rates of the order of $0.1 \text{ kg m}^{-1} \text{ s}^{-1}$. Keeping the spatial scale of 10^2 km in mind, the continuity equation for sediment transport results in an accumulation rate of the order of 1 mm a^{-1} , which is consistent with the value from isotope determinations. This demonstrates that the sediment dynamic method can be applied to determine the temporal scale of mud deposits.

Furthermore, the numerical models for hydrodynamics and sediment dynamics provide insights into the evolution of the sedimentary systems. An example is the evolution of the tidal ridges on the East China Sea continental shelf. As outlined above, these ridges are distributed in different depths (Yang 1989; Berné *et al.* 2002; Z. X. Liu *et al.* 2007). As shown in Figure 10, numerical simulations successfully reconstructed the dynamic environment for the tidal-ridge field during the Holocene (Uehara *et al.* 2002; Uehara & Saito 2003). The hydrodynamic condition in terms of palaeo-tidal currents has also been revealed by other researchers (Zhu & Chang 2000; Chen & Zhu 2012). If the sediment-transport patterns are integrated with the tidal current and seabed sediment data, then the history of the tidal-ridge system evolution can be reproduced.

From the study of Holocene deposition in the East China Sea, the diversity of depositional systems in space and time becomes apparent, indicating that the evolution of shelf sedimentary systems is not controlled by sea-level changes alone. A combination of *in situ* observations and numerical modelling will be able to establish the process-product relationship. Recently, such a forward-modelling approach for the formation of sedimentary sequences has been adopted in studies of geomorphological evolution, in addition to process studies. For the present study areas, the early Holocene deposits can be used as a test to the model output: for example, those in the Changjiang Estuary, Hangzhou Bay and the inner-shelf region off the Zhejiang–Fujian coast. The model output may be compared with the sequences, so that the

downcore ^{14}C profile (Fig. 12) may be explained in terms of the mixing between the reworked sediment and the coastal or land-derived sediment.

The nature of the Holocene sedimentary records

Continental shelf sedimentary records or archives are important in the investigations of past environmental changes (e.g. climate, sea level, seabed morphology, ecosystems). For an appropriate interpretation of the records, three criteria are important: temporal resolution, vertical continuity and time coverage. The general characteristics of the Holocene sedimentary records of the region are summarized in Table 5.

Compared with their counterparts in deep oceans, these deposits have a relatively high resolution. The temporal resolution is a function of the deposition rate and the intensity of vertical mixing (Gao & Collins, 2014). In the deep ocean, the deposition rate is often of the order of 10^{-1} – $10^{-2} \text{ mm a}^{-1}$, which may be disturbed easily by vertical material exchange induced by physical or biological processes. Thus, 1 kyr may be considered as a high resolution. However, when a temporal scale of 10 kyr (i.e. the entire Holocene) is concerned, a resolution of better than within 100 years is required. In this respect, the shelf–coastal deposits represent ideal sedimentary archives. In the areas considered here, the river deltas, tidal flats and shelf mud deposits are associated with a deposition rate of 10^1 mm a^{-1} (e.g. Gao 2009b; Fan *et al.* 2011). Thus, the resolution can be as high as 1 year (e.g. the deposits of the upper tidal flat).

The second criterion for a good sedimentary record is continuity. In many shelf–coastal systems, both accretion and erosion may occur at the same site. Extreme events, such as a typhoon storm surges, may destroy large parts of the sedimentary record. Nevertheless, the shelf mud deposits of the region tend to have relatively continuous records. In the future, numerical modelling may be used to recover missing records. For instance, based on process-orientated modelling, using the existing sedimentary records as calibration material, the environmental conditions can be reconstructed. Then, data simulation (once again, using the existing records) can be carried out in order to identify the missing parts of the record.

The third criterion for high-quality sedimentary records is the temporal coverage, or duration, of the record. Any single sedimentary record from a specific sedimentary system will cover a limited time period of the Holocene period. For example, the deposits of the abandoned Yellow River delta contain a record of 727 years, starting from AD

HOLOCENE SEDIMENTARY SYSTEMS

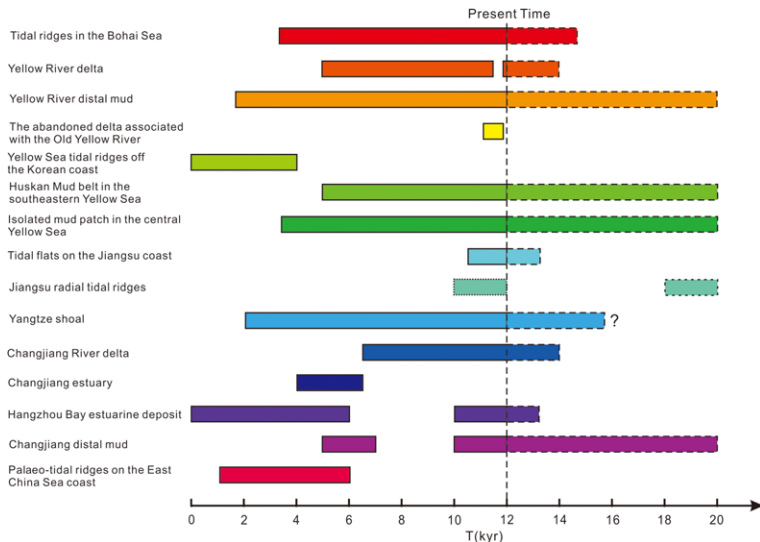


Fig. 15. Sedimentary records: present status and future evolution (based on the datasets in Table 5).

1128 and ending in AD 1855. Likewise, the distal mud deposits have different timings for their initiation, as indicated by the distal muds associated with the Yellow, Changjiang and Pearl rivers. However, these individual sedimentary records can be connected to form an integrated record covering more extensive periods.

Shelves with large widths and abundant sediment supply have the best chance of preserving complete records of the Holocene (Gao & Collins 2014). Using the available information, an attempt was made to reconstruct the temporal coverage of the various types of sedimentary records. As shown in Figure 15, it was assumed that the Holocene commenced 12 kyr ago, the beginning being marked as 0 and some future time limit as 20 kyr. Within this temporal framework, the records of the sedimentary systems described in Figure 2 cover different time periods. For the river deltas, parts of both the beginning and the final stages of the Holocene records are missing. Coastal systems such as tidal flats would be short lived because they developed over short time periods when sufficient sediment was supplied by seabed erosion or river input. The tidal-ridges systems are subjected to constant reworking; as a result, the original record formulated may be destroyed by subsequent lateral migration. In the case of the radial tidal ridges off the Jiangsu coast, less than 2 kyr have been preserved because of such lateral migration (Yin Yong pers. comm.). It is thus possible that future records will also not record more than 2 kyr. The distal mud deposits associated with large rivers, and the shelf mud patches, have the highest potential

for extended records. During the early and intermediate stages, the settling of suspended sediment provides material for continuous accumulation; during later stages, the transport mechanisms are dominated by the movement of bottom turbid layers, the presence of 'parallel clinoforms' implying continuous deposition. Therefore, these records may extend well into the future, as long as the river input continues. The prediction of the future sedimentary record is a research direction that requires further efforts. Once again, the sediment dynamics will be a useful tool for dealing with the critical issues of the timing for the onset of deposition, the spatial distribution of sedimentary systems with high-resolution records and the overall duration of sediment accumulation.

Conclusions

- In the presence of a broad shelf and abundant terrestrial sediment supply, sediment dynamic processes determine the spatial distribution and temporal evolution of the various Holocene sedimentary systems in the Bohai, Yellow and East China seas. According to the transport and accumulation processes, the Holocene deposits can be classified into different categories: deposits formed by tidal currents or combined current-wave interactions (e.g. tidal river deltas, tidal flats and tidal ridges); shelf-circulation-dominated systems, (e.g. distal muds and isolated shelf mud patches); and systems influenced by sediment gravity flow (i.e. movement of bottom

- turbid layers), as indicated by the presence of parallel clinoforms in distal mud deposits at a mature stage.
- The inherent interrelationship between the transport processes and the deposits implies that forward modelling of process–product relationships is an important research direction. Within such a framework, more and better information on aspects such as the Holocene sedimentation along the Jiangsu coast, as well as sediment sources and transport pathways for the Hangzhou Bay and Zhejiang–Fujian inner-shelf sedimentary systems during the early-middle Holocene, can be obtained. The modelling of the formation of sedimentary systems and records is an additional important scientific issue.
 - In such an environmental setting, the Holocene sedimentary systems provide ‘high-resolution time slices’ on temporal scales better than 100 years. In addition, in response to continuous sediment supply, new sedimentary systems will be formed in the future, especially shelf mud deposits. If the spatial distribution patterns of the records, which change with time, can be identified correctly, then it becomes possible to connect high-resolution time slices to generate complete Holocene sedimentary records useful in climate, environment and ecosystem change studies.

A part of the research reported here was presented at the 34th International Geological Congress (Brisbane, Australia, 5–10 August, 2012). Subsequently, the study has been financially supported by the Ministry of Science and Technology, China, through the project ‘Land–Ocean Boundary Processes and Their Impacts on the Formation of the Yangtze Deposition System’ (grant number 2013CB956500). Mr Niu Zhan-sheng is thanked for his help with the preparation of some of the figures. Professor B. W. Flemming is thanked for his comments and revision suggestions.

References

- ALEXANDER, C. R., DEMASTER, D. J. & NITTROUER, C. A. 1991. Sediment accumulation in a modern epicontinental-shelf setting: the Yellow Sea. *Marine Geology*, **98**, 51–72.
- BERNÉ, S., TRENTESAUX, A., STOLK, A., MISSIAEN, T. & DEBATIST, M. 1994. Architecture and long-term evolution of a tidal sandbank – the Middelkerke Bank (Southern North-Sea). *Marine Geology*, **121**, 57–72.
- BERNÉ, S., VAGNER, P. ET AL. 2002. Pleistocene forced regressions and tidal sand ridges in the East China Sea. *Marine Geology*, **188**, 293–315.
- BI, N. S., YANG, Z. S., WANG, H. J., HU, B. Q. & JI, Y. J. 2010. Sediment dispersion pattern off the present Huanghe (Yellow River) subdelta and its dynamic mechanism during normal river discharge period. *Estuarine, Coastal and Shelf Science*, **86**, 352–362.
- BIAN, C. W. 2012. *Chinese Coastal Sediment Transport in the Bohai Sea, Yellow Sea and East China Sea*. Doctoral thesis, Ocean University of China, 100 [in Chinese].
- BIAN, C. W., JIANG, W. S. & SONG, D. H. 2010. Terrigenous transportation to the Okinawa Trough and the influence of typhoons on suspended sediment concentration. *Continental Shelf Research*, **30**, 1189–1199.
- CHEN, B. & WANG, K. 2008. Suspended sediment transport in the offshore near Yangtze Estuary. *Journal of Hydrodynamics*, **20**, 373–381.
- CHEN, C. T. A. 2009. Chemical and physical fronts in the Bohai, Yellow and East China seas. *Journal of Marine Systems*, **78**, 394–410.
- CHEN, Q. Q. & ZHU, Y. R. 2012. Holocene evolution of bottom sediment distribution on the continental shelves of the Bohai Sea, Yellow Sea and East China Sea. *Sedimentary Geology*, **273–274**, 58–72.
- CHEN, Y. Z., SYVITSKI, J. P. M., GAO, S., OVEREEM, I. & KETTNER, A. J. 2012. Socio-economic impacts on flooding: a 4000 year history of the Yellow River, China. *AMBIO*, **41**, 682–698.
- CHEN, Z. Y. 1986. Subaqueous topography and sediments off modern Changjiang Estuary. *Donghai Marine Science*, **4**, 28–37 [in Chinese with English abstract].
- CHEN, Z. Y. & STANLEY, D. J. 1995. Quaternary subsidence and river channel migration in the Yangtze Delta Plain, Eastern China. *Journal of Coastal Research*, **11**, 927–945.
- CHOI, B. H., MUN, J. Y., KO, J. S. & YUK, J. H. 2005. Simulation of Suspended Sediment in the Yellow and East China Seas. *China Ocean Engineering*, **19**, 235–250.
- COUGH, S. K., KIM, J. W., LEE, S. H., SHINN, Y. J., JIN, J. H., SUH, M. C. & LEE, J. S. 2002. High-resolution acoustic characteristics of epicontinental sea deposits, central-eastern Yellow Sea. *Marine Geology*, **188**, 317–331.
- COUGH, S. K., LEE, H. J., CHUN, S. S. & SHINN, Y. J. 2004. Depositional processes of late Quaternary sediments in the Yellow Sea: a review. *Geosciences Journal*, **8**, 211–264.
- CHU, Z. X., SUN, X. G., ZHAI, S. K. & XU, K. H. 2006. Changing pattern of accretion/erosion of the modern Yellow River (Huanghe) subaerial delta, China: based on remote sensing images. *Marine Geology*, **227**, 13–30.
- CHUNG, Y. C. & HUNG, G. W. 2000. Particulate fluxes and transports on the slope between the southern East China Sea and the South Okinawa Trough. *Continental Shelf Research*, **20**, 571–597.
- CHUNG, Y. C., CHUNG, K., CHANG, H. C., WANG, L. W., YU, C. M. & HUNG, G. W. 2003. Variabilities of particulate flux and ^{210}Pb in the southern East China Sea and western South Okinawa Trough. *Deep-Sea Research II*, **50**, 1163–1178.
- COLLINS, M. B., SHIMWELL, S. J., GAO, S., POWELL, H., HEWITSON, C. & TAYLOR, J. A. 1995. Water and sediment movement in the vicinity of linear sandbanks: the Norfolk Banks, southern North Sea. *Marine Geology*, **123**, 125–142.
- DELEU, S., VAN LANCKER, V., VAN DEN EYNDE, D. & MOERKERKE, G. 2004. Morphodynamic evolution of the kink of an offshore tidal sandbank: the Westhinder

HOLOCENE SEDIMENTARY SYSTEMS

- Bank (Southern North Sea). *Continental Shelf Research*, **24**, 1587–1610.
- DEMASTER, D. J., MCKEE, B. A., NITTRUER, C. A., QIAN, J. C. & CHENG, G. D. 1985. Rates of sediment accumulation and particle reworking based on radiochemical measurements from continental shelf deposits in the East China Sea. *Continental Shelf Research*, **4**, 143–158.
- DING, X. R., KANG, Y. Y., MAO, Z. B., SUN, Y. L., LI, S., GAO, X. & ZHAO, X. X. 2014. Analysis of largest tidal range in radial sand ridges southern Yellow Sea. *Acta Oceanologica Sinica*, **36**, 12–20 [in Chinese with English abstract].
- DONG, L. X., GUAN, W. B., CHEN, Q., LI, X. H., LIU, X. H. & ZENG, X. M. 2011. Sediment transport in the Yellow Sea and East China Sea. *Estuarine, Coastal and Shelf Science*, **93**, 248–258.
- DOU, Y. G., YANG, S. Y. ET AL. 2010. Clay mineral evolution in the central Okinawa Trough since 28 ka: implications for sediment provenance and paleoenvironmental change. *Palaeogeography, Palaeoclimatology, Palaeoecology*, **288**, 108–117.
- DRONKERS, J. & MILTENBURG, A. G. 1996. Fine sediment deposits in shelf seas. *Journal of Marine Systems*, **7**, 119–131.
- DU, J. Z., WU, Y. F., HUANG, D. K. & ZHANG, J. 2010. Use of ^{7}Be , ^{210}Pb and ^{137}Cs tracers to the transport of surface sediments of the Changjiang Estuary, China. *Journal of Marine Systems*, **82**, 286–294.
- EVANS, G. 1965. Intertidal flat sediments and their environments of deposition in the Wash. *Quarterly Journal of the Geological Society of London*, **121**, 209–240, <http://doi.org/10.1144/gjsgs.121.1.0209>
- FAN, D. D., TU, J. B., SHANG, S. & CAI, G. F. 2014. Characteristics of tidal-bore deposits and facies associations in the Qiantang Estuary, China. *Marine Geology*, **348**, 1–14.
- FAN, D. J., QI, H. Y., SUN, X. X., LIU, Y. & YANG, Z. S. 2011. Annual lamination and its sedimentary implications in the Yangtze River delta inferred from High-resolution biogenic silica and sensitive grain-size records. *Continental Shelf Research*, **31**, 129–137.
- FENG, Y. J., LI, Y., XIE, Q. C. & ZHANG, L. R. 1990. Morphology and activity of sedimentary interfaces of the Hangzhou Bay. *Acta Oceanologica Sinica*, **12**, 213–223.
- FLEMMING, B. W. & DAVIS, R. A., JR. 1994. Holocene evolution, morphodynamics and sedimentology of the Spiekeroog Barrier Island system (southern North Sea). *Senckenbergiana Maritima*, **24**, 117–155.
- FRANK, M. 2011. Oceanography Chemical twins, separated. *Nature Geoscience*, **4**, 220–221.
- FU, M. Z. & ZHU, D. K. 1986. The sediment sources of the offshore submarine sand ridge field of the coast of Jiangsu province. *Journal of Nanjing University (Natural Sciences Edition)*, **22**, 536–544 [in Chinese with English abstract].
- GAO, S. 2007. Modeling the growth limit of the Changjiang Delta. *Geomorphology*, **85**, 225–236.
- GAO, S. 2009a. Geomorphology and sedimentology of tidal flats. In: PERILLO, G. M. E., WOLANSKI, E., CAHOON, D. & BRINSON, M. (eds) *Coastal Wetlands: an Ecosystem Integrated Approach*. Elsevier, Amsterdam, 295–316.
- GAO, S. 2009b. Modeling the preservation potential of tidal flat sedimentary records, Jiangsu coast, eastern China. *Continental Shelf Research*, **29**, 1927–1936.
- GAO, S. 2014. Sediment dynamic processes, mechanisms and evolution trends of the radial linear sandbanks, Jiangsu coast. In: WANG, Y. (ed.) *Environmental and Resource Characteristics of the Southern Yellow Sea Radial Sand Ridges*. China Ocean Press, Beijing, 275–293.
- GAO, S. & COLLINS, M. 2014. Holocene sedimentary systems on continental shelves. *Marine Geology*, **352**, 268–294.
- GAO, S. & JIA, J. J. 2003. Modeling suspended sediment distribution in continental shelf upwelling/downwelling settings. *Geo-Marine Letters*, **22**, 218–226.
- GAO, S., CHENG, P., WANG, Y. P. & CAO, Q. Y. 2000. Characteristics of suspended sediment concentrations over the areas adjacent to the Changjiang River estuary, the summer of 1998. *Marine Science Bulletin*, **2**, 14–24.
- GAO, S., WANG, Y. P. & GAO, J. H. 2011. Sediment retention at the Changjiang sub-aqueous delta over a 57 year period, in response to catchment changes. *Estuarine, Coastal and Shelf Science*, **95**, 29–38.
- GAO, S., DU, Y. F., XIE, W. J., GAO, W. H., WANG, D. D. & WU, X. D. 2014. Environment-ecosystem dynamic processes of *Spartina alterniflora* salt-marshes along the eastern China coastlines. *Science in China (Earth Sciences)*, **57**, 2567–2586.
- GRABER, H. C., BEARDSLEY, R. C. & GRANT, W. D. 1989. Storm-generated surface-waves and sediment resuspension in the East China and Yellow Seas. *Journal of Physical Oceanography*, **19**, 1039–1059.
- HAQ, B. U., HARDENBOL, J. & VAIL, P. R. 1987. Chronology of fluctuating sea levels since the Triassic. *Science*, **235**, 1156–1167.
- HONDA, M. C., KUSAKABE, M., NAKABAYASHI, S. & KATAGIRI, M. 2000. Radiocarbon of sediment trap samples from the Okinawa trough: lateral transport of ^{14}C -poor sediment from the continental slope. *Marine Chemistry*, **68**, 231–247.
- HORI, K. & SAITO, Y. 2007. An early Holocene sea-level jump and delta initiation. *Geophysical Research Letters*, **34**, L18401, <http://doi.org/10.1029/2007GL031029>
- HORI, K., SAITO, Y., ZHAO, Q. H., CHENG, X. R., WANG, P. X., SATO, Y. & LI, C. X. 2001a. Sedimentary facies and Holocene progradation rates of the Changjiang (Yangtze) delta, China. *Geomorphology*, **41**, 233–248.
- HORI, K., SAITO, Y., ZHAO, Q. H., CHENG, X. R., WANG, P. X., SATO, Y. & LI, C. X. 2001b. Sedimentary facies of the tide-dominated paleo-Changjiang (Yangtze) estuary during the last transgression. *Marine Geology*, **177**, 331–351.
- HORI, K., SAITO, Y., ZHAO, Q. H. & WANG, P. X. 2002. Architecture and evolution of the tide-dominated Changjiang (Yangtze) River delta, China. *Sedimentary Geology*, **146**, 249–264.
- HOSHIMA, A., TANIMOTO, T., MISHIMA, Y., ISEKI, K. & OKAMURA, K. 2003. Variation of turbidity and particle transport in the bottom layer of the East China Sea. *Deep-Sea Research Part II: Topical Studies in Oceanography*, **50**, 443–455.

- HSUEH, Y., SCHULTZ, J. R. & HOLLAND, W. R. 1997. The Kuroshio flow-through in the East China Sea: a numerical model. *Progress in Oceanography*, **39**, 79–108.
- HU, J. Y., KAWAMURA, H., HONG, H. S. & QI, Y. Q. 2000. A review on the currents in the South China Sea: seasonal circulation, South China Sea warm current and Kuroshio intrusion. *Journal of Oceanography*, **56**, 607–624.
- HU, K. L., DING, P. X., WANG, Z. B. & YANG, S. L. 2009. A 2D/3D hydrodynamic and sediment transport model for the Yangtze Estuary, China. *Journal of Marine Systems*, **77**, 114–136.
- HUH, C. A. & SU, C. C. 1999. Sedimentation dynamics in the East China Sea elucidated from ^{210}Pb , ^{137}Cs and $^{239,240}\text{Pu}$. *Marine Geology*, **160**, 183–196.
- HUTHNANCE, J. M. 1982a. On the formation of sand banks of finite extent. *Estuarine Coastal and Shelf Science*, **15**, 277–299.
- HUTHNANCE, J. M. 1982b. One mechanism forming linear sand banks. *Estuarine Coastal and Shelf Science*, **14**, 79–99.
- ISEKI, K., OKAMURA, K. & KIYOMOTO, Y. 2003. Seasonality and composition of downward particulate fluxes at the continental shelf and Okinawa Trough in the East China Sea. *Deep-Sea Research II: Topical Studies in Oceanography*, **50**, 457–473.
- JIA, J. J., GAO, S. & XUE, Y. C. 2003. Sediment dynamic processes of the Yuehu inlet system, Shandong Peninsula, China. *Estuarine, Coastal and Shelf Science*, **57**, 783–801.
- JIANG, W. S., POHLMANN, T., SÜNDERMANN, J. & FENG, S. Z. 2000. A modelling study of SPM transport in the Bohai Sea. *Journal of Marine Systems*, **24**, 175–200.
- JIANG, W. S., POHLMANN, T., SUN, J. & STARKE, A. 2004. SPM transport in the Bohai Sea: field experiments and numerical modeling. *Journal of Marine Systems*, **44**, 175–188.
- JIN, J. H. & COUGH, S. K. 1998. Partitioning of transgressive deposits in the southeastern Yellow Sea: a sequence stratigraphic interpretation. *Marine Geology*, **149**, 79–92.
- JIN, J. H. & COUGH, S. K. 2002. Erosional shelf sand ridges in the mid-eastern Yellow Sea. *Geo-Marine Letters*, **21**, 219–225.
- JIN, J. H., COUGH, S. K. & RVANG, W. H. 2002. Sequence aggradation and systems tracts partitioning in the mid-eastern Yellow Sea: roles of glacio-eustasy, subsidence and tidal dynamics. *Marine Geology*, **184**, 249–271.
- JIN, X. L. (ed.). 1992. *Marine Geology of the East China Sea*. China Ocean Press, Beijing [in Chinese].
- KAMP, P. J. J. & NAISH, T. 1998. Forward modelling of the sequence stratigraphic architecture of shelf cyclo-thems: application to Late Pliocene sequences, Wang-anui Basin (New Zealand). *Sedimentary Geology*, **116**, 57–80.
- LEE, H. J. & CHAO, S. Y. 2003. A climatological description of circulation in and around the East China Sea. *Deep-Sea Research II: Topical Studies in Oceanography*, **50**, 1065–1084.
- LEE, H. J. & CHU, Y. S. 2001. Origin of inner-shelf mud deposit in the southeastern Yellow Sea: Huskan Mud Belt. *Journal of Sedimentary Research*, **71**, 144–154.
- LEE, H. J. & YOON, S. H. 1997. Development of stratigraphy and sediment distribution in the northeastern Yellow Sea during Holocene sea-level rise. *Journal of Sedimentary Research*, **67**, 341–349.
- LEE, H. J., JUNG, K. T., FOREMAN, M. G. G. & CHUNG, J. Y. 2000. A three-dimensional mixed finite-difference Galerkin function model for the oceanic circulation in the Yellow Sea and the East China Sea. *Continental Shelf Research*, **20**, 863–895.
- LEE, H. J., JUNG, K. T., SO, J. K. & CHUNG, J. Y. 2002. A three-dimensional mixed finite-difference Galerkin function model for the oceanic circulation in the Yellow Sea and the East China Sea in the presence of M2 tide. *Continental Shelf Research*, **22**, 67–91.
- LI, C. X. 1986. Deltaic sedimentation. In: REN, M. E. (ed.) *Modern Sedimentation in Coastal and Nearshore Zone of China*. China Ocean Press, Beijing/Springer, Berlin, 253–378.
- LI, C. X. & LI, P. 1983. The characteristics and distribution of Holocene sand bodies in the Changjiang delta area. *Acta Oceanologica Sinica*, **2**, 54–66.
- LI, C. X. & WANG, P. 1991. Stratigraphy of the Late Quaternary barrier lagoon depositional systems along the coast of China. *Sedimentary Geology*, **72**, 189–200.
- LI, C. X., GUO, X. M., XU, S. Y., WANG, J. T. & LI, P. 1979. The characteristics and distribution of Holocene sand bodies in Changjiang, River Delta area. *Acta Oceanologica Sinica*, **1**, 252–268 [in Chinese with English abstract].
- LI, C. X., CHEN, Q. Q., ZHANG, J. Q., YANG, S. L. & FAN, D. D. 2000. Stratigraphy and paleoenvironmental changes in the Yangtze Delta during the Late Quaternary. *Journal of Asian Earth Sciences*, **18**, 453–469.
- LI, C. X., ZHANG, J. Q., FAN, D. D. & DENG, B. 2001. Holocene regression and the tidal radial sand ridge system formation in the Jiangsu coastal zone, east China. *Marine Geology*, **173**, 97–120.
- LI, C. X., WANG, P., SUN, H. P., ZHANG, J. Q., FAN, D. D. & DENG, B. 2002. Late Quaternary incised-valley fill of the Yangtze delta (China): its stratigraphic framework and evolution. *Sedimentary Geology*, **152**, 133–158.
- LI, D. Y., CHEN, J., WANG, A. J. & YU, X. G. 2009. Suspended sediment characteristics and transport in the Minjiang estuary during flood seasons. *Ocean Engineering*, **27**, 70–80 [in Chinese with English abstract].
- LI, F. Y., GAO, S., JIA, J. J. & ZHAO, Y. Y. 2002. Contemporary deposition rates of fine-grained sediment in the Bohai and Yellow Seas. *Oceanologia et Limnologia Sinica*, **33**, 364–369 [in Chinese with English Abstract].
- LI, F. Y., LI, X. G., SONG, J. M., WANG, G. Z., CHENG, P. & GAO, S. 2006. Sediment flux and source in northern Yellow Sea by ^{210}Pb technique. *Chinese Journal of Oceanology and Limnology*, **24**, 255–263.
- LI, G. X., HAN, X. B., YUE, S. H., WEN, G. Y., YANG, R. M. & KUSKY, T. M. 2006. Monthly variations of water masses in the East China Seas. *Continental Shelf Research*, **26**, 1954–1970.
- LI, H. Q., YIN, Y., SHI, Y., HE, H. C. & LIU, X. Y. 2011. Micro-morphology and contemporary sedimentation rate of tidal flat in Rudong, Jiangsu Province. *Journal*

HOLOCENE SEDIMENTARY SYSTEMS

- of Palaeogeography*, **13**, 150–160 [in Chinese with English abstract].
- LI, W., WANG, Y. H., WANG, J. N. & WEI, H. 2012. Distributions of water masses and hydrographic structures in the Yellow Sea and East China Sea in the spring and summer 2011. *Oceanologia et Limnologia Sinica*, **3**, 615–623 [in Chinese with English abstract].
- LI, Y. H., WANG, A. J., QIAO, L., FANG, J. Y. & CHEN, J. 2012. The impact of typhoon Morakot on the modern sedimentary environment of the mud deposition center off the Zhejiang–Fujian coast, China. *Continental Shelf Research*, **37**, 92–100.
- LI, Z. H., GAO, S. & CHEN, S. L. 2007. Characteristics of tide-induced bottom boundary layers over the Dafeng intertidal flats, Jiangsu Province, China. *Ocean Engineering*, **25**, 53–60 [in Chinese with English abstract].
- LIM, D. I., JUNG, H. S., CHOI, J. Y., YANG, S. & AHN, K. S. 2006. Geochemical compositions of river and shelf sediments in the Yellow Sea: grain-size normalization and sediment provenance. *Continental Shelf Research*, **26**, 15–24.
- LIM, D. I., CHOI, J. Y., JUNG, H. S., RHO, K. C. & AHN, K. S. 2007. Recent sediment accumulation and origin of shelf mud deposits in the Yellow and East China Seas. *Progress in Oceanography*, **73**, 145–159.
- LIN, C. M. 1997. Sequence stratigraphic study on the Hangzhou Bay since 15 000 a BP. *Geological Review*, **43**, 273–280 [in Chinese with English abstract].
- LIN, C. M., ZHUO, H. C. & GAO, S. 2005. Sedimentary facies and evolution in the Qiantang River incised valley, eastern China. *Marine Geology*, **219**, 235–259.
- LIN, S., HSIEH, I. J., HUANG, K. M. & WANG, C. H. 2002. Influence of the Yangtze River and grain size on the spatial variations of heavy metals and organic carbon in the East China Sea continental shelf sediments. *Chemical Geology*, **182**, 377–394.
- LIU, J., SAITO, Y., WANG, H., YANG, Z. G. & NAKASHIMA, R. 2007. Sedimentary evolution of the Holocene subaqueous clinoform off the Shandong Peninsula in the Yellow Sea. *Marine Geology*, **236**, 165–187.
- LIU, J., SAITO, Y., KONG, X. H., WANG, H., XIANG, L. H., WEN, C. & NAKASHIMA, R. 2010. Sedimentary record of environmental evolution off the Yangtze River estuary, East China Sea, during the last ~13 000 years, with special reference to the influence of the Yellow River on the Yangtze River delta during the last 600 years. *Quaternary Science Reviews*, **29**, 2424–2438.
- LIU, J., KONG, X. H., SAITO, Y., LIU, J. P., YANG, Z. S. & WEN, C. 2013. Subaqueous deltaic formation of the Old Yellow River (AD 1128–1855) on the western South Yellow Sea. *Marine Geology*, **344**, 19–33.
- LIU, J. P., MILLIMAN, J. D. & GAO, S. 2002. The Shandong mud wedge and postglacial sediment accumulation in the Yellow Sea. *Geo-Marine Letters*, **21**, 212–218.
- LIU, J. P., MILLIMAN, J. D., GAO, S. & CHENG, P. 2004. Holocene development of the Yellow River's subaqueous delta, North Yellow Sea. *Marine Geology*, **209**, 45–67.
- LIU, J. P., LI, A. ET AL. 2006. Sedimentary features of the Yangtze River-derived along-shelf clinoform deposit in the East China Sea. *Continental Shelf Research*, **26**, 2141–2156.
- LIU, J. P., XU, K., LI, A. C., MILLIMAN, J. D., VELOZZI, D. M., XIAO, S. B. & YANG, Z. S. 2007. Flux and fate of Yangtze River sediment delivered to the East China Sea. *Geomorphology*, **85**, 208–224.
- LIU, J. T. & LIN, H. L. 2004. Sediment dynamics in a submarine canyon: a case of river–sea interaction. *Marine Geology*, **207**, 55–81.
- LIU, S. F., ZHUANG, Z. Y. & LONG, H. Y. 2008. Environmental evolution and sheet sedimentation in late Quaternary in the east Bohai Sea. *Marine Geology & Quaternary Geology*, **28**, 25–31 [in Chinese with English abstract].
- LIU, S. X., SHEN, X. Q., WANG, Y. Q. & HAN, S. X. 1993. The averaged distributions and variability of water masses in the Bohai, Yellow and East China seas. *Acta Oceanologica Sinica*, **15**, 3–7 [in Chinese with English abstract].
- LIU, X. J., GAO, S. & WANG, Y. P. 2011. Modeling profile shape evolution for accreting tidal flats composed of mud and sand: a case study of the central Jiangsu coast, China. *Continental Shelf Research*, **31**, 1750–1760.
- LIU, X. Q. 1987. Relict sediments in China continental shelf. *Marine Geology & Quaternary Geology*, **7**, 1–14 [in Chinese].
- LIU, X. Y., GAO, J. H., BAI, F. L., LIU, Z. Y. & PAN, S. M. 2008. Grain size information in different evolution periods of Xinyanggang tidal flat in Jiangsu Province. *Marine Geology & Quaternary Geology*, **28**, 27–35 [in Chinese with English abstract].
- LIU, Y. L., GAO, S., WANG, Y. P., YANG, Y., LONG, J. P., ZHANG, Y. Z. & WU, X. D. 2014. Distal mud deposits associated with the Pearl River over the northwestern continental shelf of the South China Sea. *Marine Geology*, **347**, 43–57.
- LIU, Z. X. 1997. Yangtze Shoal – a modern tidal sand sheet in the northwestern part of the East China Sea. *Marine Geology*, **137**, 321–330.
- LIU, Z. X. & XIA, D. X. 2004. *Tidal Sands in the China Seas*. China Ocean Press, Beijing.
- LIU, Z. X., HUANG, Y. C. & ZHANG, Q. A. 1989. Tidal current ridges in the southwestern Yellow Sea. *Journal of Sedimentary Petrology*, **59**, 432–437.
- LIU, Z. X., XIA, D. X., TANG, Y. X., WANG, K. Y., BERNE, S., MARSSET, T. & BOURILLET, J. F. 1994. Tidal deposit system in the Eastern Bohai Sea in the Holocene. *Science in China (Series B)*, **24**, 1331–1338 [in Chinese with English abstract].
- LIU, Z. X., XIA, D. X., BERNE, S., WANG, K. Y., MARSSET, T., TANG, Y. X. & BOURILLET, J. F. 1998. Tidal deposition systems of China's continental shelf, with special reference to the eastern Bohai Sea. *Marine Geology*, **145**, 225–253.
- LIU, Z. X., BERNÉ, S., SAITO, Y., LERICOLAIS, G. & MARSSET, T. 2000. Quaternary seismic stratigraphy and paleoenvironments on the continental shelf of the East China Sea. *Journal of Asian Earth Sciences*, **18**, 441–452.
- LIU, Z. X., YIN, P., XIONG, Y. Q., BERNÉ, S., TRENTESAUX, A. & LI, C. X. 2003. Quaternary transgressive and regressive depositional sequences in the East China Sea. *Chinese Science Bulletin*, **48**, 81–87.
- LIU, Z. X., BERNÉ, S. ET AL. 2007. Internal architecture and mobility of tidal sand ridges in the East China Sea. *Continental Shelf Research*, **27**, 1820–1834.
- LIU, J., QIAO, F. L., WANG, X. H., WANG, Y. G., TENG, Y. & XIA, C. S. 2011. A numerical study of transport

- dynamics and seasonal variability of the Yellow River sediment in the Bohai and Yellow seas. *Estuarine, Coastal and Shelf Science*, **95**, 39–51.
- MARSSET, T., XIA, D., BERNÉ, S., LIU, Z., BOURILLET, J. F. & WANG, K. 1996. Stratigraphy and sedimentary environment since the Late Quaternary in the Eastern Bohai Sea. *Marine Geology*, **135**, 97–114.
- MILLIMAN, J. D., QIN, Y. S., REN, M. E. & SAITO, Y. 1987. Man's influence on the erosion and transport by Asian rivers: the Yellow River (Huanghe) example. *Journal of Geology*, **95**, 751–762.
- MILLIMAN, J. D., QIN, Y. S. & PARK, Y. A. 1989. Sediments and sedimentary processes in the Yellow and East China Seas. In: TAIRA, A. & MASUDA, F. (eds) *Sedimentary Facies in the Active Plate Margin*. Terra Scientific, Tokyo, 233–249.
- NI, W. F., WANG, Y. P., ZOU, X. Q. & GAO, J. H. 2013. Study on the sediment dynamics and stability of the Kushuiyang tidal channel at radial sand ridges in the southern Yellow Sea. *Marine Science Bulletin*, **32**, 668–677 [in Chinese with English abstract].
- NI, W. F., WANG, Y. P., ZOU, X. Q., ZHANG, J. C. & GAO, J. H. 2014. Sediment dynamics in an offshore tidal channel in the southern Yellow Sea. *International Journal of Sediment Research*, **29**, 246–259.
- NITTROUER, C. A. 1999. STRATAFORM: overview of its design and synthesis of its results. *Marine Geology*, **154**, 3–12.
- NITTROUER, C. A. & WRIGHT, L. D. 1994. Transport of particles across continental shelves. *Reviews of Geophysics*, **32**, 85–113.
- NITTROUER, C. A., AUSTIN, J. A., FIELD, M. E., KRAVITZ, J. H., SYVITSKI, J. P. M. & WIBERG, P. L. (eds). 2009. *Continental Margin Sedimentation: from Sediment Transport to Sequence Stratigraphy*. International Association of Sedimentologists, Special Publications, **37**.
- OFF, T. 1963. Rhythmic linear sand bodies caused by tidal currents. *Bulletin of the American Association of Petroleum Geologists*, **47**, 324–341.
- OGURI, K., MATSUMOTO, E., YAMADA, M., SAITO, Y. & IISEKI, K. 2003. Sediment accumulation rates and budgets of depositing particles of the East China Sea. *Deep Sea Research Part II: Topical Studies in Oceanography*, **50**, 513–528.
- OIWANE, H., TONAI, S., KIYOKAWA, S., NAKAMURA, Y., SUGANUMA, Y. & TOKUYAMA, H. 2011. Geomorphological development of the Goto Submarine Canyon, northeastern East China Sea. *Marine Geology*, **288**, 49–60.
- ORTON, G. J. & READING, H. G. 1993. Variability of deltaic processes in terms of sediment supply, with particular emphasis on grain size. *Sedimentology*, **40**, 475–512.
- PAOLA, C. 2000. Quantitative models of sedimentary basin filling. *Sedimentology*, **47** (Suppl. 1), 121–178.
- PARK, S. C. & LEE, B. H. 1994. Depositional patterns of sand ridges in tide dominated shallow water environments: Yellow Sea coast and South Sea of Korea. *Marine Geology*, **120**, 65–75.
- PARK, S. C. & YOO, D. G. 1988. Depositional history of Quaternary sediments on the continental shelf off southeastern coast of Korea (Korea Strait). *Marine Geology*, **79**, 65–75.
- PARK, S. C., YOO, D. G., LEE, K. W. & LEE, H. H. 1999. Accumulation of recent muds associated with coastal circulations, southeastern Korea Sea (Korea Strait). *Continental Shelf Research*, **19**, 589–608.
- PARK, S. C., LEE, H. H., HAN, H. S., LEE, G. H., KIM, D. C. & YOO, D. G. 2000. Evolution of late Quaternary mud deposits and recent sediment budget in the southeastern Yellow Sea. *Marine Geology*, **170**, 271–288.
- PARK, S. C., HAN, H. H. & YOO, D. G. 2003. Transgressive sand ridges on the mid-shelf of the southern sea of Korea (Korea Strait): formation and development in high-energy environments. *Marine Geology*, **193**, 1–18.
- PARK, S. C., LEE, B. H., HAN, H. S., YOO, D. G. & LEE, C. W. 2006. Late Quaternary stratigraphy and development of tidal sand ridges in the eastern Yellow Sea. *Journal of Sedimentary Research*, **76**, 1093–1105.
- PARK, Y. A., CHOI, J. Y. & GAO, S. 2001. Spatial variation of suspended particulate matter in the Yellow Sea. *Geo-Marine Letters*, **20**, 196–200.
- POSTMA, H. 1961. Transport and accumulation of suspended matter in the Dutch Wadden Sea. *Netherlands Journal of Sea Research*, **1**, 148–190.
- QIN, Y. S., ZHAO, Y. Y., CHEN, L. R. & ZHAO, S. L. (eds). 1987. *Geology of the East China Sea*. Science Press, Beijing, 290 [in Chinese].
- REN, M. E. (ed.). 1986. *Comprehensive Investigation of Coastal Zone and Tidal Flat Resources, Jiangsu Province*. China Ocean Press, Beijing [in Chinese].
- REN, M. E. 1992. Human impact on coastal landform and sedimentation – The Yellow River example. *GeoJournal*, **28**, 443–448.
- REN, M. E. 2006. Sediment discharge of the Yellow River, China: past, present and future – a synthesis. *Advance in Earth Sciences*, **21**, 551–563.
- REN, M. E. & SHI, Y. L. 1986. Sediment discharge of the Yellow River (China) and its effect on the sedimentation of the Bohai and the Yellow Sea. *Continental Shelf Research*, **6**, 785–810.
- REN, M. E., ZHANG, R. S. & YANG, J. H. 1984. Sedimentation on tidal mud flat in Wanggang area, Jiangsu Province, China. *Marine Science Bulletin*, **3**, 40–54 [in Chinese with English abstract].
- REN, M. E., ZHANG, R. S. & YANG, J. H. 1985. Effect of typhoon No.8114 on coastal morphology and sedimentation of Jiangsu Province, Peoples' Republic of China. *Journal of Coastal Research*, **1**, 21–28.
- SAITO, Y., KATAYAMA, K. ET AL. 1998. Transgressive and highstand systems tracts and post-glacial transgression, the East China Sea. *Sedimentary Geology*, **122**, 217–232.
- SAITO, Y., WEI, H. L., ZHOU, Y. Q., NISHIMURA, A., SATO, Y. & YOKOTA, S. 2000. Delta progradation and chenier formation in the Huanghe (Yellow River) Delta, China. *Journal of Asian Earth Sciences*, **18**, 489–497.
- SAITO, Y., YANG, Z. S. & HORI, K. 2001. The Huanghe (Yellow River) and Changjiang (Yangtze River) deltas: a review on their characteristics, evolution and sediment discharge during the Holocene. *Geomorphology*, **41**, 219–231.
- SCHOLL, D. W. 1964. Recent sedimentary record in mangrove swamps and rise in sea level over the southwestern coast of Florida. *Marine Geology*, **1**, 344–366.

HOLOCENE SEDIMENTARY SYSTEMS

- SHEU, D. D., HOU, W. C., CHUNG, Y. C., TANG, T. Y. & HUNG, J. J. 1999. Geochemical and carbon isotopic characterization of particles collected in sediment traps from the East China Sea continental slope and the Okinawa Trough northeast of Taiwan. *Continental Shelf Research*, **19**, 183–203.
- SHI, C., ZHANG, D. D. & YOU, L. 2003. Sediment budget of the Yellow River delta, China: the importance of dry bulk density and implications to understanding of sediment dispersal. *Marine Geology*, **199**, 13–25.
- SHI, W. & WANG, M. H. 2010. Satellite observations of the seasonal sediment plume in central East China Sea. *Journal of Marine Systems*, **82**, 280–285.
- SHI, W. & WANG, M. H. 2012. Satellite views of the Bohai Sea, Yellow Sea, and East China Sea. *Progress in Oceanography*, **104**, 30–45.
- SHI, Z. 2004. Behaviour of fine suspended sediment at the North passage of the Changjiang Estuary, China. *Journal of Hydrology*, **293**, 180–190.
- SLOSS, L. L. 1963. Sequences in the cratonic interior of North America. *Geological Society of America Bulletin*, **74**, 93–113.
- SONG, Y. H. & CHOI, M. S. 2009. REE geochemistry of fine-grained sediments from major rivers around the Yellow Sea. *Chemical Geology*, **266**, 328–342.
- STERNBERG, R. W., CACCHIONE, D. A., PAULSON, B., KINEKE, G. C. & DRAKE, D. E. 1996. Observations of sediment transport on the Amazon subaqueous delta. *Continental Shelf Research*, **16**, 697–715.
- SUN, X. P. 1995. Features of temperature-salinity of the Tushima warm current in the East China Sea in summer and differences of its salinity in the Summers of 1987 and 1989. *Journal of Oceanography of Huanghai & Bohai Seas*, **13**, 1–10 [in Chinese with English abstract].
- TRENTESAUX, A., STOLK, A. & BERNE, S. 1999. Sedimentology and stratigraphy of a tidal sand bank in the southern North Sea. *Marine Geology*, **159**, 253–272.
- UEHARA, K. & SAITO, Y. 2003. Late Quaternary evolution of the Yellow/East China Sea tidal regime and its impacts on sediments dispersal and seafloor morphology. *Sedimentary Geology*, **162**, 25–38.
- UEHARA, K., SAITO, Y. & HORI, K. 2002. Paleotidal regime in the Changjiang (Yangtze) Estuary, the East China Sea, and the Yellow Sea at 6 ka and 10 ka estimated from a numerical model. *Marine Geology*, **183**, 179–192.
- VAIL, P. R., MITCHUM, R. M. ET AL. 1977. Seismic stratigraphy and global changes of sea level. In: PAYTON, C. E. (ed.) *Seismic Stratigraphy – Applications to Hydrocarbon Exploration*. American Association of Petroleum Geologists, Memoirs, **26**, 49–212.
- WANG, A. J., PAN, S. M., ZHANG, Y. Z. & LIU, Z. Y. 2010. Modern sedimentation rate of the submarine delta of the Changjiang River. *Marine Geology & Quaternary Geology*, **30**, 1–6 [in Chinese with English abstract].
- WANG, H. J., YANG, Z. S., LI, Y. H., GUO, Z. G., SUN, X. X. & WANG, Y. 2007. Dispersal pattern of suspended sediment in the shear frontal zone off the Huanghe (Yellow River) mouth. *Continental Shelf Research*, **27**, 854–871.
- WANG, J., BAI, C. G., XU, Y. H. & BAI, S. B. 2010. Tidal couplet formation and preservation, and criteria for discriminating storm-surge sedimentation on the tidal flats of central Jiangsu Province, China. *Journal of Coastal Research*, **26**, 976–981.
- WANG, J. H., ZHOU, Y. ET AL. 2006. Late Quaternary sediments and paleoenvironmental evolution in Hangzhou Bay. *Journal of Palaeogeography*, **8**, 551–558 [in Chinese with English abstract].
- WANG, L. B., YANG, Z. S., ZHAO, X. H., XING, L., ZHAO, M. X., SAITO, Y. & FAN, D. J. 2009. Sedimentary characteristics of core YE-2 from the central mud area in the south Yellow Sea during last 8400 years and its interspace coarse layers. *Marine Geology & Quaternary Geology*, **29**, 1–11 [in Chinese with English abstract].
- WANG, X. H., QIAO, F. L., LU, J. & GONG, F. 2011. The turbidity maxima of the northern Jiangsu shoal-water in the Yellow Sea, China. *Estuarine, Coastal and Shelf Science*, **93**, 201–211.
- WANG, Y. 2014. *The Environment and Resources of Radiate Sand Ridges of South Yellow Sea*. Ocean Press, Beijing [in Chinese].
- WANG, Y. & KE, X. K. 1989. Cheniers on the east coastal plain of China. *Marine Geology*, **90**, 321–335.
- WANG, Y., ZHU, D. K., YOU, K. Y., PAN, S. M., ZHU, X. D., ZOU, X. Q. & ZHANG, Y. Z. 1999. Evolution of radiate sand ridge field of the South Yellow Sea and its sedimentary characteristics. *Science in China (Series D)*, **42**, 97–112.
- WANG, Y., ZHANG, Y. Z., ZOU, X. Q., ZHU, D. K. & PIPER, D. 2012. The sand ridge field of the South Yellow Sea: origin by river-sea interaction. *Marine Geology*, **291–294**, 132–146.
- WANG, Y. H., DONG, P., OGUCHI, T., CHEN, S. L. & SHEN, H. T. 2013. Long-term (1842–2006) morphological change and equilibrium state of the Changjiang (Yangtze) Estuary, China. *Continental Shelf Research*, **56**, 71–81.
- WANG, Y. P., ZHANG, R. S. & GAO, S. 1999. Geomorphic and hydrodynamic responses in salt marsh-tidal creek systems, Jiangsu, China. *Chinese Science Bulletin*, **44**, 544–549.
- WANG, Y. P., GAO, S., JIA, J. J., THOMPSON, C., GAO, J. H. & YANG, Y. 2012. Sediment transport over an accretional intertidal flat with influences of reclamation, Jiangsu coast, China. *Marine Geology*, **291**, 147–161.
- WANG, Y. P., VOULGARIS, G., LI, Y., YANG, Y., GAO, J. H., CHEN, J. & GAO, S. 2013. Sediment resuspension, flocculation, and settling in a macrotidal estuary. *Journal of Geophysical Research: Oceans*, **118**, 5591–5608.
- WANG, Y. Y., HE, Q. & LIU, H. 2009. Variation of near-bed suspended sediment concentration in South Passage of the Changjiang Estuary. *Journal of Sediment Research*, **6**, 6–13 [in Chinese with English abstract].
- WATANABE, M. 2007. Simulation of temperature, salinity and suspended matter distributions induced by the discharge into the East China Sea during the 1998 flood of the Yangtze River. *Estuarine, Coastal and Shelf Science*, **71**, 81–97.
- WRIGHT, L. D. & FRIEDRICH, C. T. 2006. Gravity-driven sediment transport on continental shelves: a status report. *Continental Shelf Research*, **26**, 2092–2107.

- WRIGHT, L. D., WISEMAN, W. J. ET AL. 1988. Marine dispersal and deposition of Yellow River silts by gravity-driven underflows. *Nature*, **332**, 629–632.
- WRIGHT, L. D., WISEMAN, J. R., YANG, Z. S., BORNHOLD, B. D., KELLER, G. H., PRIOR, D. B. & SUHAYDA, J. N. 1990. Processes of marine dispersal and deposition of suspended silts off the modern mouth of the Huanghe (Yellow River). *Continental Shelf Research*, **10**, 1–40.
- WRIGHT, L. D., FRIEDRICH, C., KIM, S. & SCULLY, M. 2001. Effects of ambient currents and waves on gravity-driven sediment transport on continental shelves. *Marine Geology*, **175**, 25–45.
- XIA, D. X., LIU, Z. X. & WANG, K. Y. 1995. Stratigraphy and sedimentary environments in the eastern Bohai Sea since the Late Pleistocene. *Acta Oceanologica Sinica*, **17**, 86–92 [in Chinese with English abstract].
- XIAO, S. B., LI, A. C. ET AL. 2006. Coherence between solar activity and the East Asian winter monsoon variability in the past 8000 years from Yangtze River-derived mud in the East China Sea. *Palaeogeography, Palaeoclimatology, Palaeoecology*, **237**, 293–304.
- XIE, D. F., WANG, Z. B., GAO, S. & DE VRIEND, H. J. 2009. Modeling the tidal channel morphodynamics in a macro-tidal embayment, Hangzhou Bay, China. *Continental Shelf Research*, **29**, 1757–1767.
- XING, F., WANG, Y. P. & WANG, H. V. 2012. Tidal hydrodynamics and fine-grained sediment transport on the radial sand ridge system in the southern Yellow Sea. *Marine Geology*, **291–294**, 192–210.
- XU, F. J., LI, A. C., LI, T. G., XU, K. H., CHEN, S. Y., QIU, L. W. & CAO, Y. C. 2011. Rare earth element geochemistry in the inner shelf of the East China Sea and its implication to sediment provenances. *Journal of Rare Earths*, **29**, 702–709.
- XU, K. H., MILLIMAN, J. D., LI, A. C., LIU, J. P., KAO, S. J. & WANG, S. M. 2009. Yangtze- and Taiwan-derived sediments on the inner shelf of East China Sea. *Continental Shelf Research*, **29**, 2240–2256.
- XU, K. H., LI, A. C. ET AL. 2012. Provenance, structure, and formation of the mud wedge along inner continental shelf of the East China Sea: a synthesis of the Yangtze dispersal system. *Marine Geology*, **291–294**, 176–191.
- XU, S., WANG, J. & LI, P. 1987. Developing processes and sand body features of modern Changjiang River Delta. In: YANG, Q. & XU, S. (eds) *Recent Yangtze Delta Deposits*. East China Normal University Press, Shanghai, 264–277 [in Chinese with English abstract].
- XUE, C. T. 1993. Historical changes in the Yellow River delta, China. *Marine Geology*, **113**, 321–329.
- XUE, C. T., ZHOU, Y. Q. & ZHU, X. H. 2004. The Huanghe River course and delta from end of Late Pleistocene to the 7th century BC. *Acta Oceanologica Sinica*, **26**, 48–61 [in Chinese with English abstract].
- YANG, C. & SUN, J. 1988. Tidal sand ridges on the East China Sea shelf. In: DE BOER, P. L., VAN GELDER, A. & NIO, S. D. (eds) *Tide-influenced Sedimentary Environments and Facies*. Reidel, Dordrecht, 23–38.
- YANG, C. S. 1989. Active, moribund and buried tidal sand ridges in the East China Sea and the Southern Yellow Sea. *Marine Geology*, **88**, 97–116.
- YANG, G. S., SHI, Y. F. & JI, Z. X. 2002. The morphological response of typical mud flat to sea level change in Jiangsu coastal plain. *Acta Geographica Sinica*, **57**, 76–84 [in Chinese with English abstract].
- YANG, S. Y. & YOUN, J. S. 2007. Geochemical compositions and provenance discrimination of the central south Yellow Sea sediments. *Marine Geology*, **243**, 229–241.
- YANG, S. Y., JUNG, H. S., LIMB, D. I. & LI, C. X. 2003. A review on the provenance discrimination of sediments in the Yellow Sea. *Earth-Science Reviews*, **63**, 93–120.
- YANG, S. Y., LIMB, D. I., JUNG, H. S. & OH, B. C. 2004. Geochemical composition and provenance discrimination of coastal sediments around Cheju Island in the southeastern Yellow Sea. *Marine Geology*, **206**, 41–53.
- YANG, W. D. 2002. Structure and sedimentary environment for submarine dune ridges in the East China Sea. *Marine Geology & Quaternary Geology*, **22**, 9–16.
- YANG, Z. S. & LIU, J. P. 2007. A unique Yellow River-derived distal subaqueous delta in the Yellow Sea. *Marine Geology*, **240**, 169–176.
- YANG, Z. S., JI, Y. J., BI, N. S., LEI, K. & WANG, H. J. 2011. Sediment transport off the Huanghe (Yellow River) delta and in the adjacent Bohai Sea in winter and seasonal comparison. *Estuarine, Coastal and Shelf Science*, **93**, 173–181.
- YE, Q. C. 1986. On the development of the abandoned Yellow River delta in Northern Jiangsu province. *Acta Geographica Sinica*, **41**, 112–122 [in Chinese with English abstract].
- YE, Y. C., ZHUANG, Z. Y., LAI, X. H., LIU, K. & CHEN, X. L. 2004. A study of sandy bedforms on the Yangtze Shoal in the East China Sea. *Periodical of Ocean University of China*, **34**, 1057–1062 [in Chinese with English abstract].
- YOO, D. G., LEE, C. W., KIM, S. P., JIN, H. M., KIM, J. K. & HAN, H. C. 2002. Late Quaternary transgressive and highstand systems tracts in the northern East China Sea mid-shelf. *Marine Geology*, **187**, 313–328.
- YU, L. S. 2002. The Huanghe (Yellow) River: a review of its development, characteristics, and future management issues. *Continental Shelf Research*, **22**, 389–403.
- YU, Q., WANG, Y. P., GAO, S. & FLEMMING, B. 2012. Modeling the formation of a sand bar within a large funnel-shaped, tide-dominated estuary: Qiantangjiang Estuary, China. *Marine Geology*, **299–302**, 63–76.
- YU, Q., WANG, Y. W. & GAO, S. 2014. Tide and continental shelf circulation induced suspended sediment transport on the Jiangsu coast: winter observations out of Xinyanggang. *Journal of Nanjing University (Natural Sciences Edition)*, **50**, 626–535 [in Chinese with English abstract].
- YUAN, D. L. & HSUEH, Y. 2010. Dynamics of the cross-shelf circulation in the Yellow and East China Seas in winter. *Deep-Sea Research II: Topical Studies in Oceanography*, **57**, 1745–1761.
- YUAN, D. L., ZHU, J. R., LI, C. Y. & HU, D. X. 2008. Cross-shelf circulation in the Yellow and East China Seas indicated by MODIS satellite observations. *Journal of Marine Systems*, **70**, 134–149.
- YUAN, Y., WEL, H., ZHAO, L. & JIANG, W. S. 2008. Observations of sediment resuspension and settling off the mouth of Jiaozhou Bay, Yellow Sea. *Continental Shelf Research*, **28**, 2630–2643.

HOLOCENE SEDIMENTARY SYSTEMS

- YUAN, Y. R. & CHEN, Q. 1984. Sediments and sedimentary facies of the abandoned Yellow River underwater delta in the south Yellow Sea. *Marine Geology & Quaternary Geology*, **4**, 35–43.
- ZHANG, D. S., ZHANG, J. L., ZHANG, C. K. & WANG, Z. 1998. Tidal currents develop-storm surges destroy-tidal currents restore – A preliminary explanation for the dynamic mechanism of formation and evolution of radiate sand ridges in Yellow Sea. *Science in China (Series D)*, **28**, 394–402 [in Chinese].
- ZHANG, H. F. 2013. Deposition kinetic characteristics and seabed stability analysis of Pinghai Bay, Fujian. *Journal of Applied Oceanography*, **32**, 36–45 [in Chinese with English abstract].
- ZHANG, L., LIU, Z., ZHANG, J., HONG, G. H., PARK, Y. & ZHANG, H. F. 2007. Reevaluation of mixing among multiple water masses in the shelf: an example from the East China Sea. *Continental Shelf Research*, **27**, 1969–1979.
- ZHANG, L., CHEN, S. L. & LIU, X. X. 2014. Evolution of the abandoned Huanghe (Yellow) River delta in north Jiangsu province in 800 years. *Acta Geographica Sinica*, **45**, 626–636 [in Chinese with English abstract].
- ZHANG, M. W., TANG, J. W., DONG, Q., SONG, Q. T. & DING, J. 2010. Retrieval of total suspended matter concentration in the Yellow and East China Seas from MODIS imagery. *Remote Sensing of Environment*, **114**, 392–403.
- ZHANG, R. S. 1984. Land-forming history of the Huanghe River delta and coastal plain of north Jiangsu. *Acta Geographica Sinica*, **39**, 173–184 [in Chinese with English abstract].
- ZHANG, R. S. 1992. Suspended sediment transport processes on tidal mud flat in Jiangsu Province, China. *Estuarine Coastal and Shelf Science*, **35**, 225–233.
- ZHANG, R. S. & CHEN, C. J. 1992. *A Study on the Evolution of the Jiangsu Offshore Linear Sand Ridges and the Trends of Sandbank Merging into the Intertidal Land*. China Ocean Press, Beijing [in Chinese].
- ZHANG, W. G., MA, H. L., YE, L. P., DONG, C. Y., YU, L. Z. & FENG, H. 2012. Magnetic and geochemical evidence of Yellow and Yangtze River influence on tidal flat deposits in northern Jiangsu Plain, China. *Marine Geology*, **319–322**, 47–56.
- ZHANG, X., LIN, C. M., DALRYMPLE, R. W., GAO, S. & LI, Y. L. 2014. Facies architecture and depositional model of a macrotidal incised-valley succession (Qiantang River estuary, eastern China), and differences from other macrotidal systems. *Geological Society of America Bulletin*, **126**, 499–522.
- ZHANG, X. X., WANG, W. W., YAN, C. C., YAN, W. B., DAI, Y. X., XU, P. & ZHU, C. X. 2014. Historical coastline spatio-temporal evolution analysis in Jiangsu coastal area during the past 1000 years. *Scientia Geographica Sinica*, **34**, 344–351 [in Chinese with English abstract].
- ZHAO, Y. Y., GAO, S., WANG, D. D., XU, Z., ZHU, D. & WANG, X. F. 2014. Characteristics and formation mechanisms of the rhythmic morphology of salt-marsh edge cliffs. *Acta Geographica Sinica*, **69**, 378–390 [in Chinese with English abstract].
- ZHU, C., CHENG, P., LU, C. C. & WANG, W. 1996. The evolution analysis on Yangtze River delta and the coastal areas of northern Jiangsu Province, since 7000 years ago. *Scientia Geographica Sinica*, **16**, 207–213 [in Chinese].
- ZHU, C., XUE, B., PAN, J. M., ZHANG, H. S., WAGNER, T. & PANCOST, R. D. 2008. The dispersal of sedimentary terrestrial organic matter in the East China Sea (ECS) as revealed by biomarkers and hydro-chemical characteristics. *Organic Geochemistry*, **39**, 952–957.
- ZHU, D. K. & XU, T. G. 1982. Wetland evolution and management issues of the central Jiangsu coast. *Journal of Nanjing University (Natural Sciences Edition)*, **18**, 799–818 [in Chinese with English abstract].
- ZHU, D. K. & AN, Z. S. 1993. Formation and Evolution of radial sand ridges in Jiangsu offshore zones. In: *Paper Collection of Geography on Celebrating 80th Birthday of Prof. Ren Mei-e*. Nanjing University Press, Nanjing, 142–147 [in Chinese].
- ZHU, D. K., KE, X. K. & GAO, S. 1986. Tidal flat sedimentation of Jiangsu coast. *Oceanography of Huanghai and Bohai Seas*, **4**, 19–27 [in Chinese with English abstract].
- ZHU, D. K., MARTINI, L. P. & BROOKFIELD, M. E. 1998. Morphology and land-use of coastal zone of the north Jiangsu Plain, Jiangsu Province, eastern China. *Journal of Coastal Research*, **14**, 591–599.
- ZHU, Y. & CHANG, R. 2000. Preliminary study of the dynamic origin of the distribution pattern of bottom sediments on the continental shelves of the Bohai Sea, Yellow Sea and East China Sea. *Estuarine, Coastal and Shelf Science*, **51**, 663–680.